Precambrian Research 244 (2014) 170–191

Contents lists available at ScienceDirect

Precambrian Research

journal homepage: www.elsevier.com/locate/precamres

# Paleomagnetic and geochemical studies of the Mesoproterozoic Satakunta dyke swarms, Finland, with implications for a Northern Europe – North America (NENA) connection within Nuna supercontinent

J. Salminen[a,*], S. Mertanen[b], D.A.D. Evans[a], Z. Wang[a]

[a] Department of Geology and Geophysics, Yale University, 301 Kline Geology Laboratory, P.O. Box 208109, New Haven, CT 06520-8109, USA
[b] Geological Survey of Finland, Laboratory for Paleomagnetism, P.O. Box 96, FI-02151 Espoo, Finland

ARTICLE INFO

*Article history:*
Received 9 January 2013
Received in revised form 12 August 2013
Accepted 26 August 2013
Available online 5 September 2013

*Keywords:*
NENA
Nuna
Late Mesoproterozoic
Subjotnian
Paleomagnetism
Rock magnetism

ABSTRACT

The existence of the Paleoproterozoic supercontinent Nuna (Columbia, Hudsonland) has been proposed by several authors. Many recent reconstructions of this supercontinent are based on the assumption that Baltica and Laurentia form part of its core in a Northern Europe – North America (NENA) configuration. The E–W, N–S and NE–SW trending Early Mesoproterozoic diabase dyke swarms in Satakunta, SW Finland, provide new paleomagnetic data to test the NENA configuration. A high-inclination, secondary remanence component carried by maghemite was isolated from some sites, and is interpreted to record hydrothermal alteration during the initial Mesozoic breakup of Pangea. A dual-polarity, high-stability remanence component was found in about half of the studied sites, and confirmed to be primary by several positive baked-contact tests. A suite of rock-magnetic analyses demonstrates that pseudo-single domain magnetite is the remanence carrier. The combined mean direction for N–S (1565 Ma; Lehtonen et al., 2003) and NE–SW trending dykes, showing both polarities, is $D = 11.5^\circ$, $I = 3.3^\circ$ ($\alpha_{95} = 8.8^\circ$), yielding a key paleomagnetic pole (SK1) for Baltica at 29.3° N, 188.1° E ($A_{95} = 6.6^\circ$). It fulfills the first six of seven Van der Voo's (1990) reliability criteria for paleomagnetic poles. The new Satakunta SK1 pole, when compared to the nearly coeval Western Channel Diabase pole (1590 ± 4 Ma) from Laurentia, allows the NENA fit at 1.57–1.59 Ga. Based on geological evidence E–W dykes have been proposed to belong a swarm that is ca. 100 million years older than the N–S dykes. E–W trending dykes show a dual polarity direction of $D = 356.9^\circ$, $I = 8.3^\circ$ ($\alpha_{95} = 15.9^\circ$), yielding a paleomagnetic pole (SK2) for Baltica at 32.6° N, 205.5° E ($A_{95} = 14.3^\circ$). Based on coeval paleomagnetic data and correlations of geochronology and basement geology of Baltica and Laurentia, the NENA fit is validated at 1.77–1.75 Ga, 1.59–1.57 Ga, 1.46 Ga, and 1.27 Ga, and by comparing single virtual geomagnetic poles at 1.63 Ga. However, the mean 1.63 Ga data from Laurentia (Melville Bugt dykes, Greenland; Halls et al., 2011) and Baltica (Sipoo dykes, Finland) are offset by about 30°. Validation of NENA for both older and younger times suggests to us that a variety of factors, such as less than highest-quality or not coeval paleomagnetic data, possible unrecognized tilting of the continental blocks, or a non-symmetric geomagnetic field, other than cratonic reconstruction, can explain the minor 1.63 Ga mean pole discordance.



## 1. Introduction

The concept of supercontinent cyclecity is established mainly based on the global peaks in distribution of zircon U–Pb and whole rock Nd-model ages (Condie, 1998, 2004). Reddy and Evans (2009) recently summarized the secular evolution of Earth from the Neoarchean to the Mesoproterozoic Eras, revealing intriguing temporal relationships of the supercontinent cycles with evolution of Earth's core, mantle, crust, oceans, atmosphere, and life. For example, the temporal distribution of rapakivi magmatism worldwide at 2.8–2.6 Ga, 1.8–1.0 Ga, and 1.0–0.5 Ga could be coeval with supercontinent cycles (e.g. Rämö and Haapala, 1995; Condie, 1998; Åhäll et al., 2000; Haapala et al., 2005; Larin, 2009). In southeastern Fennoscandia, the rapakivi granite batholiths represents the silicic member of a bimodal magmatic complex, in which tholeiitic diabase dykes and minor gabbroic-anorthositic bodies

* Corresponding author. Present address: Department of Geophysics and Astronomy, Physics Department, University of Helsinki, P.O. Box 64, FIN-00014 University of Helsinki, Finland. Tel.: +358 9 191 51013; fax: +358 919151000.
*E-mail addresses:* johanna.m.salminen@helsinki.fi (J. Salminen), satu.mertanen@gtk.fi (S. Mertanen), david.evans@yale.edu (D.A.D. Evans), zhengrong.wang@yale.edu (Z. Wang).

0301-9268/$ – see front matter 
http://dx.doi.org/10.1016/j.precamres.2013.08.006

represent the mafic member (Lindberg and Eklund, 1992; Haapala and Rämö, 1992; Eklund et al., 1994). Paleomagnetism of these Late Mesoproterozoic formations that are commonly called Subjotnian (ca. 1.65–1.54 Ga) in Fennoscandia have been widely-studied (e.g. Neuvonen and Grundström, 1969; Neuvonen, 1970, 1978, 1986; Bylund, 1985; Pesonen, 1987; Pesonen et al., 1987, 1991; Bylund and Elming, 1992; Mertanen and Pesonen, 1995; Mertanen et al., 2008). However, a closer look at these data shows that many of them are scattered with large and overlapping 95% confidence circles ($A_{95}$) about the calculated mean paleomagnetic poles, and only a few of these poles come from rock formations that have been radiometrically dated and whose magnetization has been proven to be primary. Our aim of this study is to fill in the gaps of the paleomagnetic record with a new, well-defined Subjotnian paleomagnetic pole for Baltica.

A basic assumption for paleomagnetic research is that when averaged over a sufficient geological time interval (~$10^4$ to $10^5$ years), the Earth's magnetic field may be approximated by geocentric axial dipole (GAD, e.g. Hospers, 1954; Irving, 1964, 2005). However, its existence during Precambrian must be tested (e.g. Evans, 2006). Support for dynamo activity since the Late Archean–Early Proterozoic began when Smirnov and Tarduno (2004) pointed out that the magnitude of secular variation at ca. 2.5 Ga (recorded by dykes from Superior and Karelia) was already similar to the present one. More recent work by Biggin et al. (2008) and Smirnov et al. (2011) showed that the dynamo was already working at 2.5 Ga, and although geomagnetic secular variation during the Late Archean and Early Proterozoic was different from that of the past 200 million years, the Mid-Proterozoic interval had already become similar to the modern. Moreover, Evans (2006) showed that the GAD model fits the distribution of evaporite basins on Earth throughout most of the last two billion years, indicating that GAD should be valid for Subjotnian times.

The existence of the Paleoproterozoic supercontinent Nuna (Columbia, Hudsonland) has been proposed by several previous studies (e.g., Williams et al., 1991; Hoffman, 1996; Meert, 2002; Rogers and Santosh, 2002; Zhao et al., 2002; Pesonen et al., 2003; Condie, 2004). Baltica (East European craton) and east Laurentia (North America and Greenland) are thought to represent two of the most important building blocks of this supercontinent. The temporal and compositional overlap of the anorogenic and orogenic magmatism between west Baltica and east Laurentia, as well as the paleomagnetic data available, suggest that these continents coexisted for more than 600 Ma (from ca. 1.2 to 1.8 Ga), constituting so called 'NENA' (Northern Europe – North America; Gower et al., 1990). A rather limited paleomagnetic dataset in the last century supported a NENA-like Mesoproterozoic reconstruction (Patchett et al., 1978; Piper, 1980) that was either static (Buchan et al., 1990) or internally shearing (Pesonen et al., 2003). More recent data have appeared to support, within the analytical uncertainties, a single NENA juxtaposition between Baltica and Laurentia between ca. 1750 and ca. 1270 Ma (Salminen and Pesonen, 2007; Evans and Pisarevsky, 2008; Lubnina et al., 2010; Pisarevsky and Bylund, 2010; Evans and Mitchell, 2011; Pesonen et al., 2012), and perhaps lasting as long as ca. 1120 Ma (Salminen et al., 2009; Raiskila et al., 2011) and forming the core of Nuna. Moreover, Nuna might include other continents, such as Siberia (e.g. Wingate et al., 2009; Evans and Mitchell, 2011), Amazonia (Bispo-Santos et al., 2008, 2012; Johansson, 2009), Australia (e.g. Hoffman, 1991; Karlstrom et al., 2001; Betts et al., 2008; Payne et al., 2009), and North China (Halls et al., 2000; Wu et al., 2005; Kusky et al., 2007; Zhang et al., 2012). Many of these reconstructions are based on the assumption that Baltica and Laurentia form the core of Nuna in a configuration similar to NENA. However, recent paleomagnetic data from ca. Melville Bugt dykes (1.63 Ga) in Greenland does not support that fit (Halls et al., 2011). To address these concerns, we present here new key and other well defined paleomagnetic pole from the Satakunta mafic dyke swarms (one dyke U–Pb dated at 1565 Ma; Lehtonen et al., 2003) from the West coast of southern Finland and suggest that NENA was also valid at 1.63–1.57 Ga. Based on the trending at the field, geochemical and paleomagnetic data we divided studied Satakunta Subjotnian dykes in two swarms: (1) E–W and (2) combined N–S and NE–SW.

## 2. Geological setting

Most continental crusts in the southern Finland were formed during the Svecofennian (a.k.a. Svecokarelian) orogeny at ca. 1.9–1.8 Ga (Huhma, 1986), related to an oblique collision of a growing Svecofennian island arc system against the Archean craton and to the subsequent continental deformation, metamorphism and crust-forming magmatism (e.g., Korja et al., 2006; Lahtinen et al., 2008). The post-collisional uplift at 1.8 Ga ended the Svecofennian orogeny. About 200 Ma later, the region entered into phases of a long period of crustal extension, development of rift basins, and anorogenic magmatism, including intrusion of several mafic dykes and sills (Eklund and Shebanov, 2005; Andersson et al., 2006). These magmatic units have been traditionally divided into three main groups based on their age relationship to the rift-filling ("Jotnian") sandstones: Subjotnian (ca. 1.65–1.54 Ga), Jotnian, and Postjotnian (ca. 1.25 Ga). Subjotnian units are exposed in the southern part of Finland (Fig. 1) such that the younger units seem to be exposed in the SW part of Finland (e.g. Åland, Vehmaa, and Laitila) and the older in the SE part of Finland (e.g. Wiborg, Suomenniemi, and Häme; Fig. 1). However a recent detailed mineralogical study of ovoids from the Vehmaa rapakivi (SW Finland; Fig. 1) batholith by Shebanov et al. (2000) showed that core zones of these ovoids give a U–Pb (zircon) age of 1630 Ma, and the matrix gives a U–Pb (zircon) age of 1573 Ma. These data indicate that in SW Finland there is a deep Subjotnian assemblage that gives the same age as the E–W dyke swarm and the SE Finnish rapakivi batholiths, proposed as a continuous Subjotnian magmatic province (Shebanov et al., 2000). Furthermore, both chemical and mineralogical compositions provide evidence for magma mixing between the rapakivi and mafic magmas, indicating that the emplacement of Subjotnian rapakivi batholiths were coeval with the intrusion of the dykes (Lindberg and Eklund, 1992; Eklund et al., 1994).

In Satakunta, the Svecofennian crust consists of Paleoproterozoic granitoids, paragneisses and felsic and intermediate metavolcanic rocks (Fig. 2). This assemblage is cut by several Subjotnian rapakivi granite intrusions and mafic dyke swarms trending E–W, N–S and NE–SW belonging in different age groups. We did not observe and there are no reports of Postjotnian diabase dykes exposed near our sampling sites (e.g. Pihlaja, 1987; Lehtonen et al., 2003; Suominen et al., 2006). Based on petrography, mode of occurrence, and field relations, it has been suggested that the Subjotnian dykes in Satakunta are continuations of both the ESE–WNW trending Häme dyke swarm (1646 ± 6 Ma: U–Pb (zr), Laitakari, 1987 and 1667 ± 9 Ma: Vaasjoki and Sakko, 1989) and the SSW–NNE trending Föglö dyke swarm (1577 ± 12 Ma: U–Pb (bd + zr) and 1540 ± 12 Ma, Suominen, 1991) (Fig. 1). The widths of the Subjotnian swarms are tens of kilometers, and the lengths are likely ca. 300 km. The dykes dip vertically or subvertically. Dyke widths vary from a few centimeters to over one hundred meters. One of the presently studied N–S trending dykes has a baddeleyite U–Pb age of ca. 1565 Ma (Lehtonen et al., 2003), suggesting that it belongs to the same system as the Föglö dykes. Lehtonen et al. (2003) obtained discordant ($^{207}Pb/^{206}Pb$) age results with three age series of ~1476, 1513, and 1565 Ma. Since the two first results were so close to each other, basically forming one point, no error estimation was possible. The

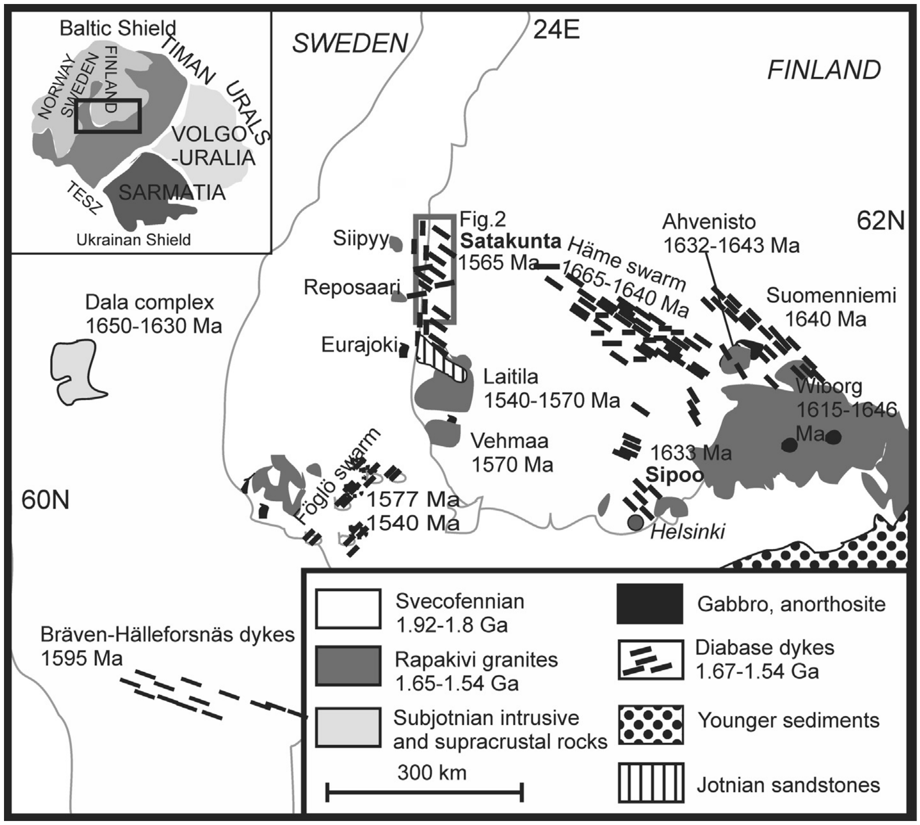


**Fig. 1.** Simplified geological map of Southern Fennoscandian shield.

Modified after Rämö (1991).

zircon upper intercept age is ca. 1.59 Ga, supporting the Subjotnian age for the dyke. Lehtonen et al. (2003) interpreted that the $^{207}$Pb/$^{206}$Pb age of 1565 Ma best represents the time of crystallization.

Pihlaja (1987) and Lehtonen et al. (2003) studied petrography of these dykes. The major mineral phases include plagioclase, hypersthene, augite, and olivine. Accessory minerals are apatite, ilmenite, magnetite, and sometimes sulfides. Some of the Subjotnian dykes in Finland are highly altered with hydrothermal mineral replacement (e.g. epidote, calcite, and sericite) (Ehlers and Ehlers, 1977; Pihlaja, 1987; Mänttäri et al., 2005; Paulamäki et al., 2006; Mertanen, 2008).

## 3. Samples and methods

### 3.1. Sampling

Altogether, forty-one diabase dyke sites were sampled at Satakunta, Finland, spanning ca. 100 km from the northernmost sampling site to the southernmost sampling site (Fig. 2). The sampling area is located north of the Satakunta sandstone (see Klein et al., in this volume) and Postjotnian mafic intrusions. From thirty-one sites we sampled baked host rocks, and from twenty-two of them the unbaked host rock was sampled for baked contact tests to study the origin of magnetic remanence (Everitt and Clegg, 1962). In thirty-one of the sites, standard oriented cores were collected with a portable field drill, in seven of the sites both oriented core and block samples were taken, and in three sites only oriented block samples were taken. Cored samples were oriented using both sun and magnetic compasses, whereas block samples were oriented using only a magnetic compass.

### 3.2. Magnetic measurements

Paleomagnetic measurements were conducted in the magnetically shielded room of the paleomagnetic laboratory of the Department of Geology and Geophysics at the Yale University, USA. After the measurement of natural remanent magnetization (NRM), samples were placed into liquid nitrogen in a null field to demagnetize viscous remanent magnetization (Borradaile et al., 2004). Thereafter, the majority of samples were thermally demagnetized to separate the characteristic remanent magnetization (ChRM) component. A few sister specimens were stepwise demagnetized using the alternating field (AF) method. The thermal method turned out to be more effective and provided more stable results than the AF method. Remanent magnetization was measured using an automated sample-changing system attached to a 2G cryogenic magnetometer (Kirschvink et al., 2008). A nitrogen-atmosphere ASC Scientific model TD-48SC furnace was used for thermal demagnetization. The demagnetization results were analyzed using orthogonal plots, stereographic projections, and demagnetization decay curves (Zijderveld, 1967) and calculated using principal component analysis (Kirschvink, 1980; Jones, 2002). Components with a minimum of four demagnetization steps were used to calculate vector lines using least-square fits, and an upper limit for maximum angular deviation (MAD) less than 6° was used as a quality filter. In a few samples directions with MAD up to 10° were accepted (from sites KA, OJ, PL, RK, SA, VR) for components interpreted to be overprints. Mean remanence directions were calculated using Fisher statistics (Fisher, 1953). Data was not streaked toward any overprinted directions except slightly in sites AM and AT, but results obtained using Fisher statistics are similar as those using Bingham statistics (Onstott, 1980).

Magnetic mineralogy was investigated by several methods using selected powdered whole-rock samples. Susceptibility

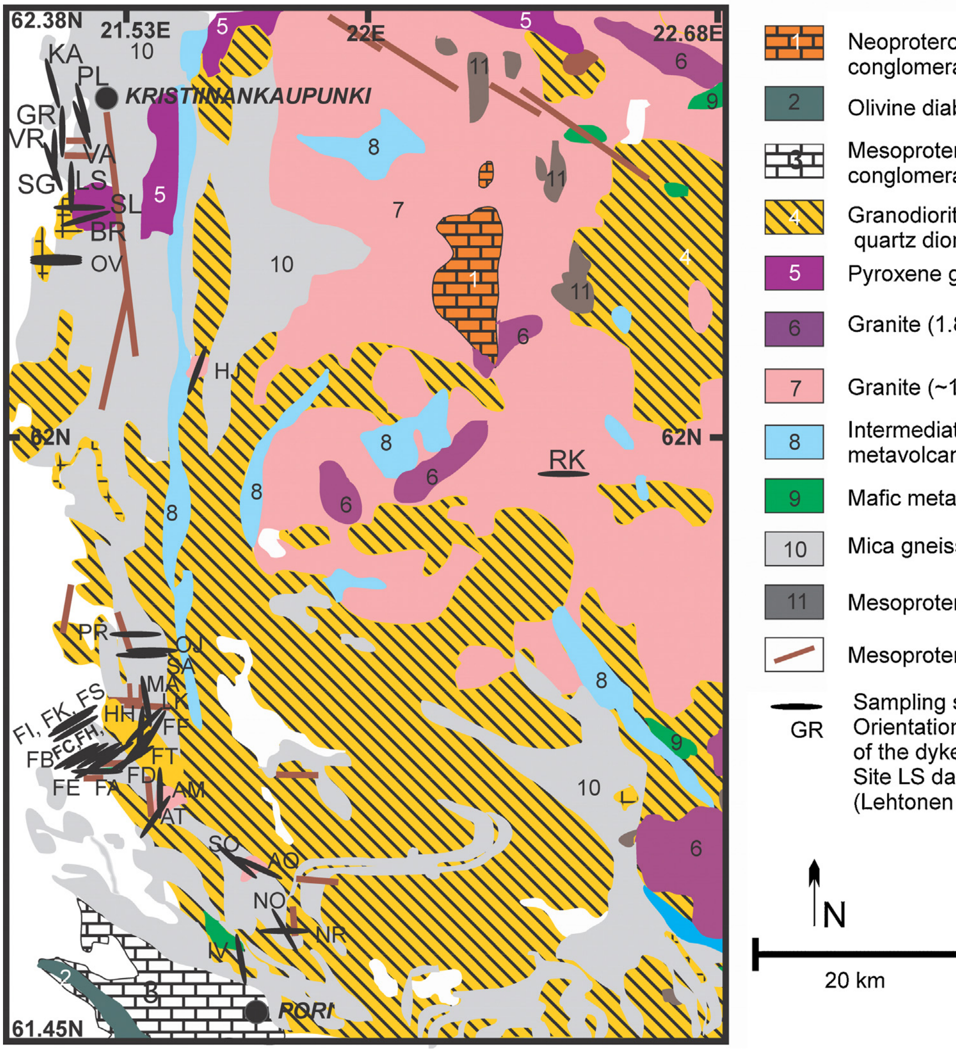


**Fig. 2.** Geological map of the study area with the location of sampling sites. Modified after Korsman et al. (1997).

measurements at both low and high temperature were done at Yale University using AGICO's KLY4-CS Kappabridge instruments to characterize magnetic carriers in the samples. The low-temperature experiment, in which samples were heated from −194 °C to room temperature (RT, 25 °C), was carried out first. Then, the same samples were heated from RT to 700 °C and cooled back to RT in argon gas which helped to avoid oxidation of minerals during the high-temperature experiments. AGICO's Kappabridge was used to measure the anisotropy of magnetic susceptibility (AMS). The technique of Jelinek (1981) was used for statistical analyses of AMS data. Room-temperature hysteresis properties were measured to determine domain states of magnetic carriers at the Institute for Rock Magnetism (IRM), University of Minnesota, USA, using a vibrating sample magnetometer (from Princeton Measurements Corporation). Low-temperature remanence measurements to explore magnetic carriers were conducted at IRM using a magnetic properties measurement system (MPMS) superconducting quantum interference device (SQUID) magnetometer (from Quantum Design, Inc.).

### 3.3. Geochemical sample processing and measurements

Trace element, rare earth element (REE), and Pb-isotope compositions of bulk samples were analyzed at Yale University. Small rock chips from the fresh parts of samples in the middle of the unheated paleomagnetic core were ground using hand operated iron mill. All sample processing was performed in a clean room of the Yale University. About 0.1–0.15 g of sample powders were weighed and dissolved at 100 °C for over 12 h in a high-pressure digestion system using 4:1 HF + $HClO_4$ + trace amount of $HNO_3$ in a Teflon beaker under the pressure about 2 bar. After total dissolution the sample solution was dried by slowly raising the temperature from 100 to 210 °C, in order to evaporate residual HF, $SiF_4$, and $HClO_4$. After the samples are completely dried, 6.2 N HCl was added and samples were dried again at 210 °C. This procedure was repeated three times, during the last time of which, a drop of $H_2O_2$ was added to adjust oxygen fugacity. After samples are completely dried, 4.0 ml of 6.2 N HCl was used to dissolve the sample.

A small aliquot of the samples were dried down again, nitrified by 3 N $HNO_3$, and then dissolved in 5% $HNO_3$ with 2 ppb Indium (as an internal standard) for measuring trace metal and REE element concentrations using ICP-MS (Element-XR) at Yale University. The reference material BHVO-2 (basalt from Pahoehoe lava from Halemaumau, Hawaii, USA) issued by United States Geological Survey (USGS) was used as a standard. The typical precision for trace metal and REE elements analyses is better than ±3%.

An aliquot of samples (about 0.08–0.1 g) were processed for Pb-isotope analyses. All samples were first passed through an

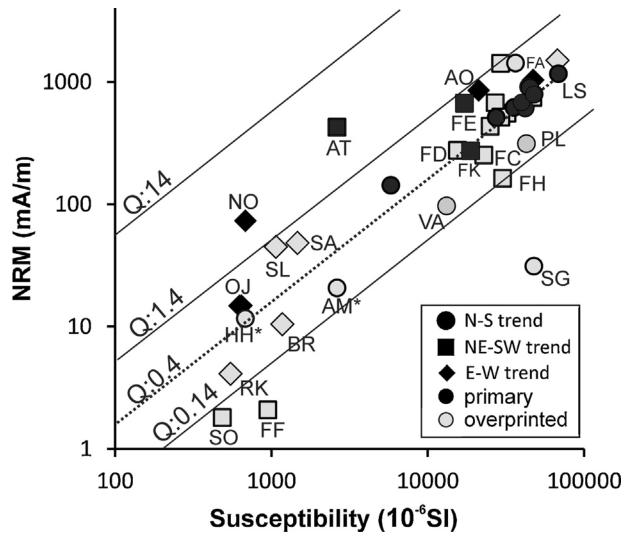


**Fig. 3.** Remanence-susceptibility (logarithmic scale) diagrams for Satakunta (Finland) dyke samples. Koenigsberger's *Q* ratios (calculated with the field value of 50 μT) are shown as straight lines. Dykes showing shallow primary component P are marked with black and dykes showing overprint secondary component S are marked with gray. *Dykes from site have been divided to two groups and this is the group with lower NRM values (see Table 1).

anion exchange column to separate Fe from other elements (AG1-X8 anion resin, Biorad column, 0.5 cm OD and 3.0 cm long). Pb isotopes were separated from the portion without Fe using the HBr–$HNO_3$ procedure similar to Abouchami et al. (1999). The typical blank for this protocol is <5 pictogram. Pb isotope compositions were measured using multi-collector ICP-MS (Neptune) at Yale University. The SRM997 Tl was used as an internal standard for mass-bias correction ($^{203}Tl/^{205}Tl = 0.418923$), and typical external reproducibility (including full chemistry) are ~12 ppm (2$\sigma$) for $^{207}Pb/^{206}Pb$, ~16 ppm (2$\sigma$) for $^{208}Pb/^{206}Pb$, ~0.002 (2$\sigma$) for $^{206}Pb/^{204}Pb$, ~0.0016 (2$\sigma$) for $^{207}Pb/^{204}Pb$, and ~0.004 (2$\sigma$) for $^{208}Pb/^{204}Pb$, comparable with other studies (e.g., Hart and Blusztajn, 2006).

## 4. Results

### 4.1. Petrophysics and paleomagnetism

Petrophysical properties are presented in Table 1 and Fig. 3. The intensity of the remanence of dyke samples ranges from 2 to 1500 mA/m. Susceptibility of the samples ranges from 550 × $10^{-6}$ SI to 68,600 × $10^{-6}$ SI. The wide range of remanence intensity and susceptibility values is probably caused by variation in the grain sizes and/or degree of weathering. Koenigsberger's *Q* value is the ratio of the remanent magnetization to the induced magnetization in the Earth's magnetic field. *Q* values of Satakunta dykes range from 0.1 to 3 (Fig. 3 *Q* values lower than 0.4 are commonly associated with overprinted or unstable magnetization).

Stable paleomagnetic directions were obtained from thirty-two sites (Table 2). We identified three components from the Subjotnian dyke samples: (1) a shallow north component and its reversed direction with high unblocking-temperature hereafter called 'primary component P' (Figs. 4 and 5); (2) a steep downward ENE component hereafter called secondary component S (Fig. 6); and (3) a steep downward and northerly component of viscous origin that shows Present day Earth's magnetic Field (PEF) direction ($D = 7°$, $I = 74°$). Component P was obtained from seventeen sites, among which six samples also show component S (i.e. AM, AO, FA, FE, IV, MA). In these cases component S was observed only in samples near the centers of the dykes or further away from the margins

**Table 1**
Site mean petrophysical properties of the Satakunta mafic dykes.

| Site | *n* | NRM (mA/m) | Susceptibility ($10^{-6}$ SI) | *Q* | Site | *n* | NRM (mA/m) | Susceptibility ($10^{-6}$ SI) | *Q* | Site | *n* | NRM (mA/m) | Susceptibility ($10^{-6}$ SI) | *Q* |
|---|---|---|---|---|---|---|---|---|---|---|---|---|---|---|
| N–S trending dykes | | | | | NE–SW trending dykes | | | | | E–W trending dykes | | | | |
| AM[a] | 8 | 21 ± 16 | 2635 ± 2150 | 0.2 ± 0.04 | AT | 4 | 110 ± 1018 | 2481 ± 7 | 0.7 ± 0.28 | AO | 6 | 854 ± 243 | 21220 ± 1024 | 0.9 ± 0.32 |
| AM | 6 | 910 ± 398 | 44137 ± 16522 | 0.5 ± 0.22 | FB | 5 | 555 ± 250 | 32228 ± 5158 | 0.3 ± 0.07 | BR | 5 | 10 ± 3 | 1179 ± 60 | 0.2 ± 0.07 |
| GR | 6 | 660 ± 314 | 40363 ± 9248 | 0.4 ± 0.18 | FC | 3 | 253 ± 167 | 22857 ± 4684 | 0.3 ± 0.22 | FA | 8 | 1039 ± 301 | 47470 ± 8503 | 0.5 ± 0.16 |
| HH[a] | 2 | 12 ± 3 | 681 | 0.4 ± 0.1 | FD | 6 | 277 ± 188 | 15530 ± 10000 | 0.3 ± 0.08 | NE, NI, NM | 11 | 15 ± 15 | 645 ± 92 | 0.6 ± 0.54 |
| HH | 5 | 143 ± 101 | 5817 ± 2184 | 0.9 ± 0.42 | FE | 7 | 671 ± 507 | 17168 ± 12693 | ±0.65 | NO | 8 | 73 ± 70 | 684 ± 65 | 3.1 ± 2.51 |
| HJ | 15 | 1425 ± 644 | 36408 ± 7035 | 0.9 ± 0.42 | FF | 3 | 2 ± 265 | 949 ± 762 | ±2.7 | NR | 8 | 1501 ± 532 | 67684 ± 13568 | 0.6 ± 0.28 |
| IV | 10 | 514 ± 104 | 27371 ± 5177 | 0.4 ± 0.09 | FH | 3 | 163 ± 72 | 30190 ± 5670 | 0.2 ± 0.05 | OJ | 6 | 15 ± 5 | 627 ± 195 | 0.7 ± 0.34 |
| KA | 6 | 747 ± 203 | 46998 ± 4894 | 0.4 ± 0.08 | FI | 6 | 677 ± 258 | 26970 ± 3427 | 0.6 ± 0.17 | RK | 7 | 4 ± 2 | 550 ± 37 | 0.2 ± 0.08 |
| LS | 5 | 1170 ± 272 | 68596 ± 4171 | 0.4 ± 0.09 | FK | 13 | 274 ± 201 | 18805 ± 22019 | 0.7 ± 0.39 | SA | 5 | 48 ± 22 | 1470 ± 140 | 0.7 ± 0.37 |
| MA | 9 | 797 ± 275 | 47997 ± 1223 | 0.4 ± 0.12 | FS | 7 | 434 ± 176 | 25065 ± 3985 | 0.4 ± 0.08 | SL | 5 | 45 ± 11 | 1073 ± 60 | 1.0 ± 0.25 |
| OV | 9 | 618 ± 250 | 35690 ± 14316 | 0.4 ± 0.12 | FT | 13 | 517 ± 305 | 29351 ± 12627 | 0.5 ± 0.22 | | | | | |
| PL | 7 | 313 ± 186 | 42713 ± 9121 | 0.2 ± 0.09 | LK | 6 | 1422 ± 426 | 29310 ± 10130 | 1.7 ± 1.07 | | | | | |
| SG | 5 | 31 ± 9 | 47698 ± 5671 | 0.01 ± 0.01 | SO | 4 | 2 ± 1 | 485 ± 33 | 0.1 ± 0.04 | | | | | |
| VA | 6 | 97 ± 55 | 13202 ± 2526 | 0.1 ± 0.08 | | | | | | | | | | |
| VR | 5 | 614 ± 157 | 42078 ± 6658 | 0.3 ± 0.04 | | | | | | | | | | |

*n* is the number of samples; *Q* is the Koenigsberger's ratio calculated for a field of 50 μT; the standard deviations are for each site.
[a] These samples showed one to two order of magnitude lower NRM values than other samples from the same site.

**Table 2**
Paleomagnetic results from Satakunta dykes and host rocks.

| Site | Rock type | Lat(° N)/logn(° E) | Str(°)/dip(°) | Width (m) | *D* (°) | *I* (°) | $\alpha_{95}$ (°) | *k* | Plat (° N) | Plong (° E) | $A_{95}$ (°) | *K* | *n* | Pol |
|---|---|---|---|---|---|---|---|---|---|---|---|---|---|---|
| **Primary component P** | | | | | | | | | | | | | | |
| *N–S* | | | | | | | | | | | | | | |
| AM | Dyke | 61.662/21.620 | 360/90 | >20 | 2.6 | −4.2 | 20.3 | 8.4 | 26.1 | 198.7 | 11.3 | 24.9 | 8 | N |
| HJ | Dyke | 62.059/21.670 | 20/90 | 10 | 15.9 | 17.0 | 9.0 | 19.2 | 35.5 | 182.0 | 8.7 | 20.4 | 15 | N |
| IV | Dyke | 61.542/21.752 | 350/90 | 20 | 27.2 | 18.7 | 18.7 | 17.6 | 34.4 | 168.2 | 18.3 | 18.4 | 5 | N |
| LS | Dyke | 62.206/21.429 | 360/? | >60 | 33.9 | 36.1 | 10.9 | 49.8 | 42.4 | 156.4 | 8.7 | 77.4 | 5 | N |
| MA | Dyke | 61.726/21.609 | 350/90 | 15 | 22.1 | 15.0 | 15.2 | 14.3 | 33.9 | 174.4 | 11.8 | 22.8 | 8 | N |
| AM | Baked granite | 61.662/21.620 | | | 21.4 | −6.0 | | | 23.3 | 178.2 | | | 2 | N |
| HJ | Baked granite | 62.059/21.680 | | | 22.8 | 6.5 | 24.0 | 15.6 | 28.8 | 175.4 | 21.9 | 18.6 | 4 | N |
| IV | Baked gneiss | 61.542/21.752 | | | 28.0 | 25.5 | 42.2 | 9.6 | 38.1 | 167.1 | 43.6 | 9.1 | 3 | N |
| GR[a] | Dyke | 62.240/21.380 | 360/60 | 1.5 | 171.2 | −12.1 | 22.5 | 12.5 | −33.6 | 32.0 | 22.1 | 12.9 | 5 | R |
| OV1[a] | Dyke | 62.154/21.395 | 10/60 | 0.15 | 186.9 | 36.2 | 25.9 | 23.7 | −6.7 | 15.6 | 21.9 | 32.6 | 3 | R |
| OV2[a] | Dyke | 62.154/21.395 | 10/60 | 0.05 | 188.7 | 13.1 | 12.3 | 101.1 | −20.8 | 12.1 | 11.3 | 120.7 | 3 | R |
| OV3[a] | Dyke | 62.154/21.395 | 10/60 | 0.015 | 189.0 | 13.8 | 11.4 | 117.2 | −20.4 | 11.9 | 6.9 | 324.1 | 3 | R |
| GR[a] | Dyke | 62.240/21.380 | 360/60 | 1.5 | 171.2 | −12.1 | 22.5 | 12.5 | −33.6 | 32.0 | 22.1 | 12.9 | 5 | R |
| GR[a] | Baked gneiss | 62.240/21.380 | | | 183.2 | 3.6 | | | 25.9 | 197.8 | | | 1 | R |
| OV[a] | Baked gneiss | 62.154/21.395 | | | 174.8 | 5.1 | | | −25.2 | 27.1 | | | 1 | R |
| Mean N–S | | | | | 13.1 | 3.7 | 11.4 | 13.0 | 29.2 | 186.2 | 8.2 | 24.6 | 15*/71 | N, R |
| *NE–SW* | | | | | | | | | | | | | | |
| AT | Dyke | 61.644/21.635 | 35/90 | 0.1 | 348.7 | 12.8 | 30.0 | 10.3 | 34.7 | 216.1 | 21.5 | 19.3 | 4 | N |
| FE | Dyke | 61.679/21.545 | 60/72 | 0.3 | 28.3 | 3.1 | 29.3 | 10.8 | 26.4 | 169.6 | 22.6 | 17.5 | 4 | N |
| AT | Baked granite | 61.644/21.635 | | | 8.3 | −3.5 | | | 26.3 | 192.4 | | | 1 | N |
| Additional sites from Mertanen, 2008 | | | | | | | | | | | | | | |
| $DS_p$ | Dyke | 61.243/21.479 | 60/70 | 1.5 | 5.5 | −0.1 | 6.4 | 90.6 | 28.4 | 195.2 | 5.6 | 116.2 | 1/7*/17 | N |
| $DB_p$ | Dyke | 61.224/21.508 | 66/90 | 0.06 | 4.6 | −0.7 | 13.9 | 19.8 | 28.6 | 196.2 | 10.7 | 32.9 | 1/7*/7 | N |
| Mean NE–SW | | | | | 6.8 | 3.9 | 20.0 | 22.1 | 30.3 | 193.7 | 19.0 | 24.2 | 5*/33 | N |
| *SK1: mean N–S and NE–SW* | | | | 11.5 | 3.3 | 8.8 | 15.5 | 29.3 | 188.1 | 6.6 | 26.6 | 20*/104 | N, R | |
| *E–W* | | | | | | | | | | | | | | |
| AO | Dyke | 61.607/21.783 | 295/60 | 0.25 | 12.8 | 5.3 | 7.1 | 73.3 | 30.3 | 186.9 | 6.3 | 94.2 | 7 | N |
| NO | Dyke | 61.560/21.820 | 330/65 | 0.6 | 349.7 | 8.4 | 35.5 | 7.7 | 32.2 | 214.1 | 35.4 | 7.7 | 4 | N |
| OJ | Dyke | 61.744/21.616 | 270/90 | 0.1 | 351.5 | 21.8 | 4.9 | 58.1 | 40.6 | 212.7 | 5.0 | 55.2 | 16 | N |
| AO | Baked granite | 61.607/21.783 | | | 10.5 | −1.0 | 23.2 | 11.8 | 27.4 | 190.0 | 21.6 | 13.5 | 5 | N |
| FA[a] | Dyke | 61.679/21.545 | 270/90 | 0.35 | 159.4 | −6.2 | 33.7 | 14.5 | −29.6 | 44.9 | 29.4 | 18.6 | 3 | R |
| *SK2: mean E–W* | | | | 356.9 | 8.3 | 15.9 | 24.2 | 32.6 | 205.5 | 14.3 | 29.8 | 5*/35 | N, R | |
| *Unbaked SVF direction* | | | | | | | | | | | | | | |
| AM | Granite | 61.662/21.620 | | | 334.6 | 60.2 | | | 65.5 | 250.3 | | | 2 | N |
| FA | Migmatite | 61.679/21.545 | | | 354.6 | 49.7 | | | 58.6 | 210.5 | | | 1 | N |
| HJ | Granite | 62.059/21.690 | | | 356.1 | 49.3 | | | 58.0 | 208.0 | | | 1 | N |
| SL | Granitoid | 62.197/21.441 | | | 318.6 | 34.8 | | | 38.4 | 254.3 | | | 1 | N |
| **Secondary component S** | | | | | | | | | | | | | | |
| AM | Dyke | 61.662/21.620 | 360/90 | >20 | 033.5 | 56.0 | 12.4 | 13.2 | 57.4 | 146.3 | 14.5 | 9.9 | 12 | N |
| AO | Dyke | 61.607/21.783 | 295/60 | 0.25 | 27.3 | 47.1 | 41.9 | 3.0 | 52.1 | 160.7 | 42.8 | 2.9 | 7 | N |
| FA | Dyke | 61.679/21.545 | 270/90 | 0.35 | 40.3 | 59.3 | 29.2 | 3.4 | 57.5 | 134.3 | 38.1 | 2.4 | 11 | N |
| FB[b] | Dyke | 61.683/21.550 | 240/? | 1 | 353.8 | 69.3 | 17.1 | 16.4 | 80.6 | 225.1 | 26.9 | 7.2 | 6 | N |
| FC | Dyke | 61.680/21.550 | 60/90 | 7 | 92.4 | 59.8 | 41.2 | 5.9 | 34.9 | 095.7 | 60.5 | 3.3 | 4 | N |
| FD | Dyke | 61.680/21.546 | 60/50 | 0.3 | 84.6 | 57.0 | 38.3 | 6.7 | 66.3 | 064.7 | 54.0 | 3.9 | 4 | N |
| FE | Dyke | 61.679/21.545 | 60/72 | 0.3 | 022.4 | 76.1 | 19.4 | 7.2 | 79.6 | 090.8 | 30.9 | 3.4 | 10 | N |
| FH | Dyke | 61.681/21.546 | 60/80 | 0.3 | 57.4 | 80.2 | 19.3 | 41.9 | 29.6 | 060.0 | 35.6 | 13.0 | 3 | N |
| FI | Dyke | 61.687/21.594 | 60/90 | 0.2 | 124.1 | 66.7 | 12.2 | 31.0 | 29.1 | 104.8 | 18.4 | 14.3 | 6 | N |
| FK | Dyke | 61.680/21.542 | 58/90 | 0.8 | 80.8 | 47.3 | 35.5 | 13.1 | 34.0 | 087.6 | 42.7 | 9.4 | 3 | N |
| FS | Dyke | 61.680/21.542 | 50/90 | 0.35 | 102.5 | 58.7 | 16.2 | 14.9 | 28.7 | 080.8 | 22.3 | 8.3 | 7 | N |
| IV | Dyke | 61.542/21.752 | 350/90 | 20 | 24.0 | 62.1 | 18.5 | 8.7 | 66.9 | 152.7 | 26.2 | 4.8 | 9 | N |
| MA | Dyke | 61.726/21.609 | 350/90 | 15 | 43 | 52.8 | 29.4 | 10.8 | 50.7 | 137.6 | 42.6 | 5.6 | 4 | N |

Table 2 (*Continued*)

| Site | Rock type | Lat(° N)/logn(° E) | Str(°)/dip(°) | Width (m) | $D$ (°) | $I$ (°) | $\alpha_{95}$ (°) | $k$ | Plat (° N) | Plong (° E) | $A_{95}$ (°) | $K$ | $n$ | Pol |
|---|---|---|---|---|---|---|---|---|---|---|---|---|---|---|
| NR | Dyke | 61.560/21.820 | 275/85 | 0.2 | 85.1 | 46.1 | 35.3 | 2.3 | 26.2 | 102.0 | 38.1 | 2.1 | 13 | N |
| RK | Dyke | 61.975/22.333 | 270/90 | 4 | 53.0 | 62.8 | 11.5 | 45.5 | 54.9 | 117.6 | 16.7 | 22.0 | 5 | N |
| SA | Dyke | 61.744/21.616 | 270/75 | ? | 56.3 | 83.4 | 20.3 | 9.8 | 66.5 | 49.7 | 34.6 | 4.0 | 7 | N |
| VA[c] | Dyke | 62.269/21.434 | 340/90 | 15 | 33.6 | 29.3 | 15.8 | 24.5 | 37.8 | 159.1 | 12.2 | 40.4 | 5 | N |
| *Mean* | | | | | 62.6 | 64.3 | 8.9 | 19.4 | 53.3 | 103.9 | 13.2 | 9.4 | 15*/110 | N |

lat/long – sampling latitude and longitude, Str/dip – strike and dip of the dyke, width – width of dyke, $D$ – declination, $I$ – inclination, $\alpha$ – the radius of the 95% confidence cone in Fisher (1953) statistics, Plat/Plong – paleolatitude/paleolongitude of the pole, $A_{95}$ – radius of the 95% confidence cone of the VGP, $K$ – Fisher precision parameter, $(N)/n$ – number of analyzed (sites)/samples, * – the number used to calculate mean value, pol – polarity of the isolated direction: $N(R)$ – normal (reversed) polarity.

[a] Reversed directions are inverted for grand mean. SVF – Svecofennian.

[b] Not in mean.

[c] These are originally of Svecofennian aged dykes.

(larger grain size) of host rocks and dykes. One site LS (age 1565 Ma; Lehtonen et al., 2003) gave a remanence direction between P and the PEF/S-clusters (Fig. 7). Stable component S and/or PEF were obtained from seventeen sites. Three sites (SL, RK, and VR) show WNW downward directions close to the well-known Svecofennian paleomagnetic direction. Due to the higher degree of metamorphism at site SL, it was noted in the field that the dyke may be of Svecofennian age. Since in this study we are concentrating on Mesoproterozoic dykes, these results are not further discussed. It is worth noting that one sample from dyke VR shows component P as an overprint on the Svecofennian direction, which we speculate as a possible thermochemical overprint by a nearby Mesoproterozoic dyke that is not exposed.

#### 4.1.1. *Primary component P*

In general, similar characteristic remanence directions with unblocking temperatures from 500 °C to 585 °C for component P were isolated from all dykes regardless of the dyke trend. Both N–S and E–W trending dykes show two polarities whereas NE–SW trending dykes show only normal-polarity directions. We employed the standard convention of assigning “normal” polarity to north-directed ChRM vectors from Proterozoic rocks in Baltica; relating this arbitrary definition to the absolute sense of Mesoproterozoic geomagnetic polarity is uncertain due to the lack of continuity in the Baltica APWP through Neoproterozoic ages. The trajectories in Zijderveld diagrams pass through the origin, indicating that there is no higher-temperature component present in the samples.

Full baked contact tests were obtained from two sites (AM and HJ) of N–S trending dykes (Figs. 8 and 9, respectively). At these sites, dykes and baked host rocks gave component P, and unbaked Svecofennian-aged host rocks showed the expected Svecofennian direction. Unblocking temperatures for component P in baked host rocks are 450–585 °C. In addition to these fully constrained baked contact tests, component P was obtained at several sites (AO, AT, GR, IV, and OV) from baked host rocks (e.g. Fig. 4), but unbaked host rocks at these sites were unstable during demagnetization. Reversed polarity components were obtained for both dykes and baked host rocks from sites OV and GR (for example Fig. 4c and d). Table 2 presents a summary of paleomagnetic results, and site mean directions for component P are shown in Fig. 10. Because field observations indicate that E–W trending dykes are older than N–S and NE–SW trending dykes, we have combined mean values for component P in respect to the trend of dykes. The combined mean direction for N–S and NE–SW trending dykes, plus two additional NE–SW sites from Mertanen (2008), has parameters $D = 11.5°$, $I = 3.3°$ (20 sites, $\alpha_{95} = 8.8°$) and yields a dual-polarity paleomagnetic pole located at Plat = 29.3° N, Plong = 188.1° E ($A_{95} = 6.6°$). The mean value for E–W trending dykes is $D = 356.9°$, $I = 8.3°$ (5 sites, $\alpha_{95} = 15.9°$) and yields a dual-polarity paleomagnetic pole located at Plat = 32.6° N, Plong = 205.5° E ($A_{95} = 14.3°$).

At the dated site LS (1565 Ma, Lehtonen et al., 2003) the interior of the dyke (with a width > 60 m) was sampled since the contacts were not exposed. Due to large mineral grains, more than half of the NRM intensity was lost during the liquid nitrogen treatment. At the beginning of demagnetization a strong PEF direction was observed, which persisted until 560 °C. Then, an intermediate steep direction was observed before samples were fully demagnetized at 583 °C (Fig. 7), which is somewhat steeper than the P component separated from the other dykes, but within a reasonable expectation for the secular variation of the geomagnetic field. Thus, the site is included in the P mean calculations (Fig. 10).

#### 4.1.2. *Secondary component S*

A steep-down, secondary component S with ENE declination was isolated from half of the sites, in temperature ranges from

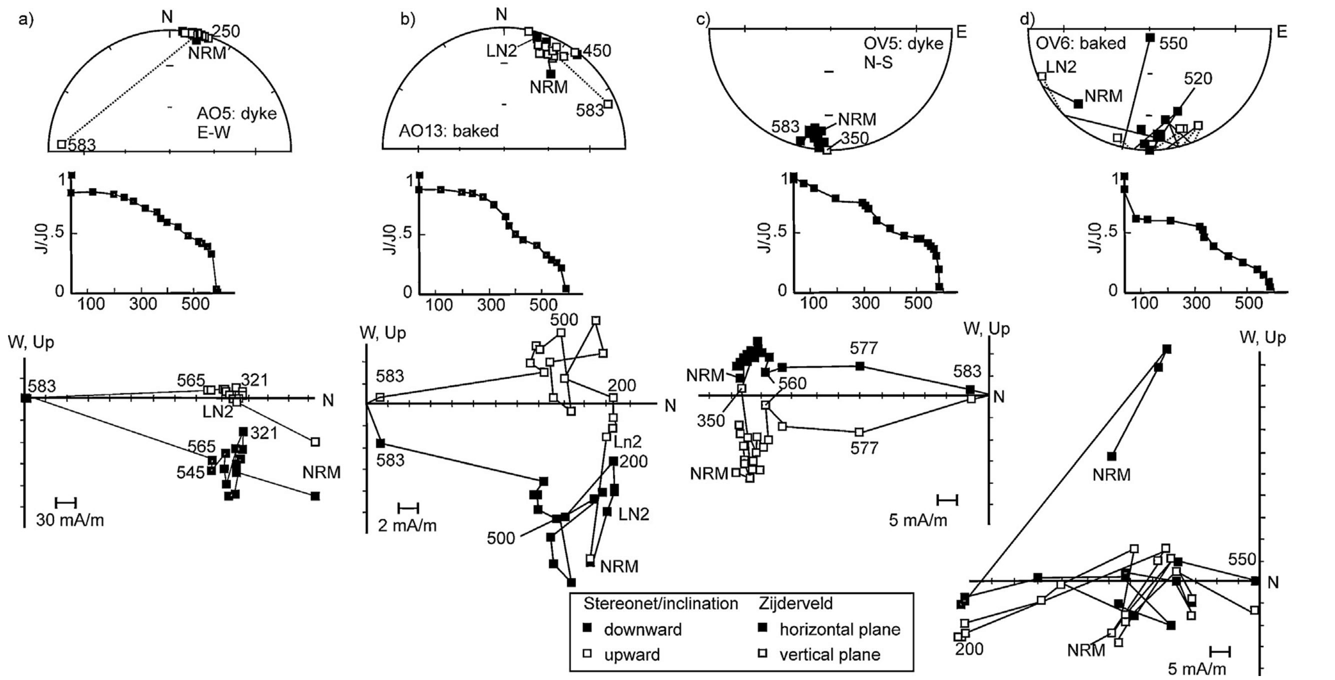


**Fig. 4.** Example of thermal demagnetization of E–W trending dyke showing primary component P. Figures show stereographic projection, normalized intensity curve ($J/J_0$) and orthogonal projections of remanent magnetization directions. (a) Normal polarity direction obtained from dyke trending E–W, (b) normal polarity direction obtained from baked host rock sample, (c) reversed polarity direction from dyke trending N–S, and (d) reversed polarity direction from baked host rock sample. Figures show stereographic projection, normalized intensity curve ($J/J_0$) and orthogonal projections of remanent magnetization directions.

300 °C to 585 °C (Figs. 6 and 11). It was mainly obtained from NE–SW trending dykes, which are more altered than other dykes (e.g. Pihlaja, 1987), and from coarse grained and/or weathered samples being more vulnerable to remagnetization. In some cases distinction between PEF and component S was not clear. The mean direction for component S is $D = 62.6°$, $I = 64.3°$ with $\alpha_{95} = 8.9°$ and it yields a paleomagnetic pole located at Plat = 53.3° N, Plong = 103.9° E ($A_{95} = 13.2°$) (Table 2).

### 4.2. Magnetic mineralogy

Observed Curie points and Verwey transition temperatures are listed in Table 3, and representative thermomagnetic (susceptibility versus temperature) curves are shown in Fig. 12. In most samples, high-temperature thermomagnetic curves showed two Curie temperatures. The higher Curie temperatures ($T_{C2}$) range from 574 °C to 584 °C in curves showing pronounced Hopkinson's peaks which have the typical feature of stable SD/PSD magnetite (Dunlop and Özdemir, 1997). Presence of magnetite is also supported by the well-characterized Verwey-transition at ~120 K during both susceptibility and remanent magnetization measurements. The lower-temperature Curie point and remanent magnetization measurements indicate the presence of maghemite, titanomagnetite or pyrrhotite. The majority of samples was saturated below 0.4 T during hysteresis measurements (Fig. 13; Table 3) supporting magnetite as the dominant magnetic mineral (O'Reilly,

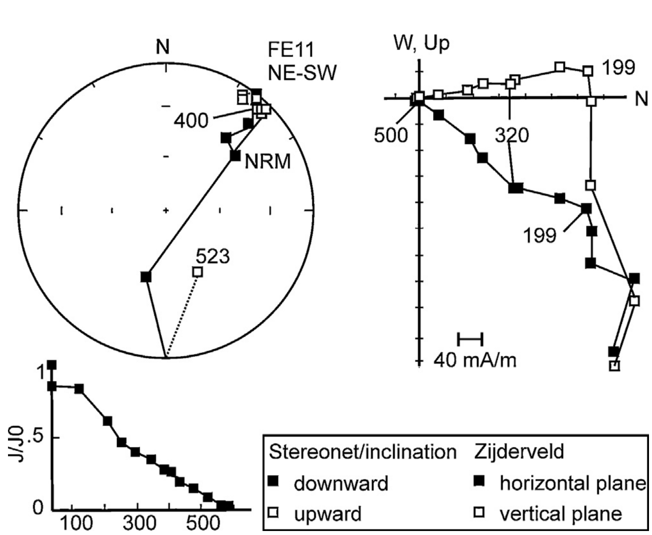


**Fig. 5.** Example of thermal demagnetization of NE–SW trending dyke showing primary component P. Figures show stereographic projection, normalized intensity curve ($J/J_0$) and orthogonal projections of remanent magnetization directions.

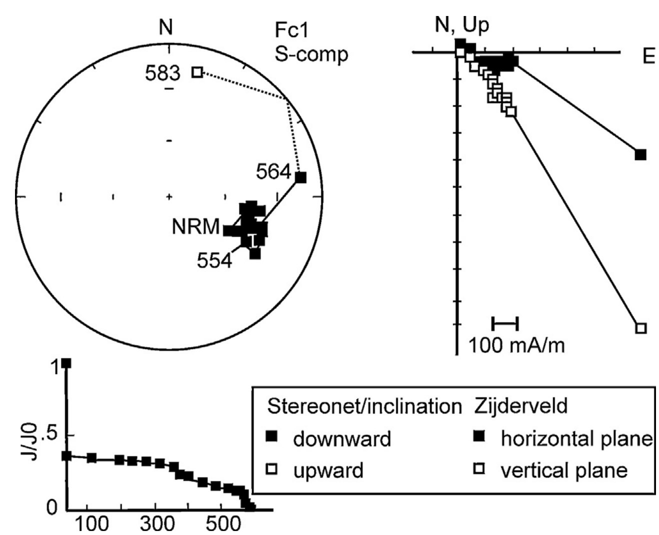


**Fig. 6.** Example of thermal demagnetization of NE–SW trending dyke showing secondary component S. Figures show stereographic projection, normalized intensity curve ($J/J_0$) and orthogonal projections of remanent magnetization directions.

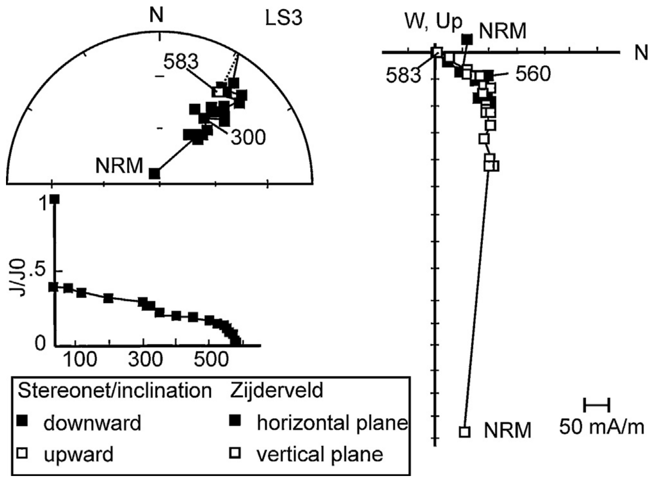


**Fig. 7.** Example of thermal demagnetization of the N–S trending dated dyke LS (1565 Ma; Lehtonen et al., 2003) showing a clear present earth field direction (PEF) component and also the primary component P. This sample is coarse grained and therefore carries strong PEF component.

1984; Dekkers, 1988). In the modified Day-plot (Day et al., 1977; Dunlop, 2002), most samples occur in the pseudo-single-domain (PSD) region (Fig. 13).

### 4.3. Anisotropy of magnetic susceptibility

The degree of anisotropy of magnetic susceptibility (AMS) ($P = K_{max}/K_{min}$) is low, and the shape parameter data are equally distributed showing both prolate and oblate signatures (Fig. 14) indicating that the characteristic remanent magnetization direction is not significantly affected by later deformation (Hrouda, 1982). In the studied dykes the magnetic foliation plane ($K_{max} - K_{int}$) agrees with the strike of the dykes (Fig. 15), indicating "normal" fabric (e.g. Knight and Walker, 1988; Rochette et al., 1992, 1999; Ernst and Baragar, 1992; Tauxe et al., 1998; Raposo et al., 2004; Raposo, 2011). This fabric has usually been interpreted to reflect the direction of magma flow, and the $K_{max}$ inclination has been used to infer the relative position between magma source and dykes themselves (e.g. Knight and Walker, 1988; Raposo et al., 2004; Raposo, 2011). In some cases when unstable paleomagnetic directions or strong secondary components were observed (Fig. 15c), the magnetic foliation plane disagrees with the strikes of dykes (e.g. Fig. 15), most probably indicating later alteration processes.

### 4.4. Geochemistry

Fig. 16 shows that Nb concentrations of Satakunta dykes are within the range defined by other Subjotnian mafic dykes in Finland (e.g. Luttinen and Kosunen, 2006). Incompatible element ratios (Nb/Y) of Satakunta N–S and NE–SW trending dykes are similar to those of Subjotnian dykes in Åland (1.57–1.54 Ga), whereas Nb/Y ratios of E–W trending dykes show similarities to those of Häme dykes (1.67–1.64 Ga). These results support the grouping based on paleomagnetic data. The wide range of Nb/Y values (Table 2) indicates different geochemical features of the primary melts of these dikes (differences in the degree of melting and crustal contamination, and/or source compositions). Because Nb/Y ratios of the melt vary little during magma differentiation, the low Nb/Y values of the Satakunta N–S and NE–SW dykes and Åland dykes indicate they could originate from the same mantle source, but represent higher degree of melt compared with other Subjotnian mafic formations Table 4.

The grouping of Satakunta dykes based on their trend is also supported by Pb isotope compositions (Fig. 17, $^{207}Pb/^{204}Pb$ versus $^{206}Pb/^{204}Pb$ plot of Satakunta and Sipoo whole-rock mafic dyke samples). Both groups form isochrons, supporting the notion of closed systems. Combined Satakunta E–W and Sipoo Subjotnian

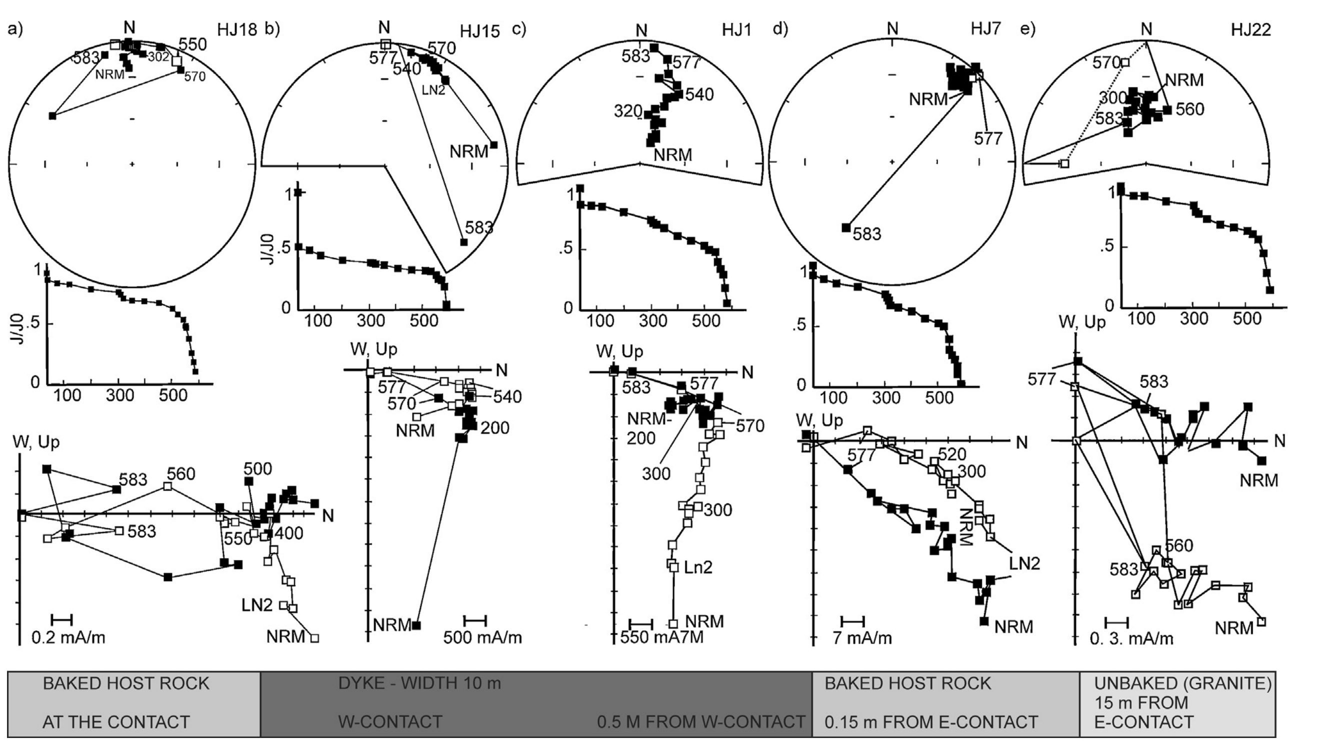


**Fig. 8.** Positive baked contact test for samples from the Satakunta N–S trending dyke (HJ), and its baked and unbaked granitic host rock. (a) Granite from right next to W-contact of the dyke, (b) dyke sample right at the E-contact, (c) dyke sample 0.5 m from contact, (d) baked host granite 0.15 m from W-contact, and (e) unbaked granite 15 m from contact.

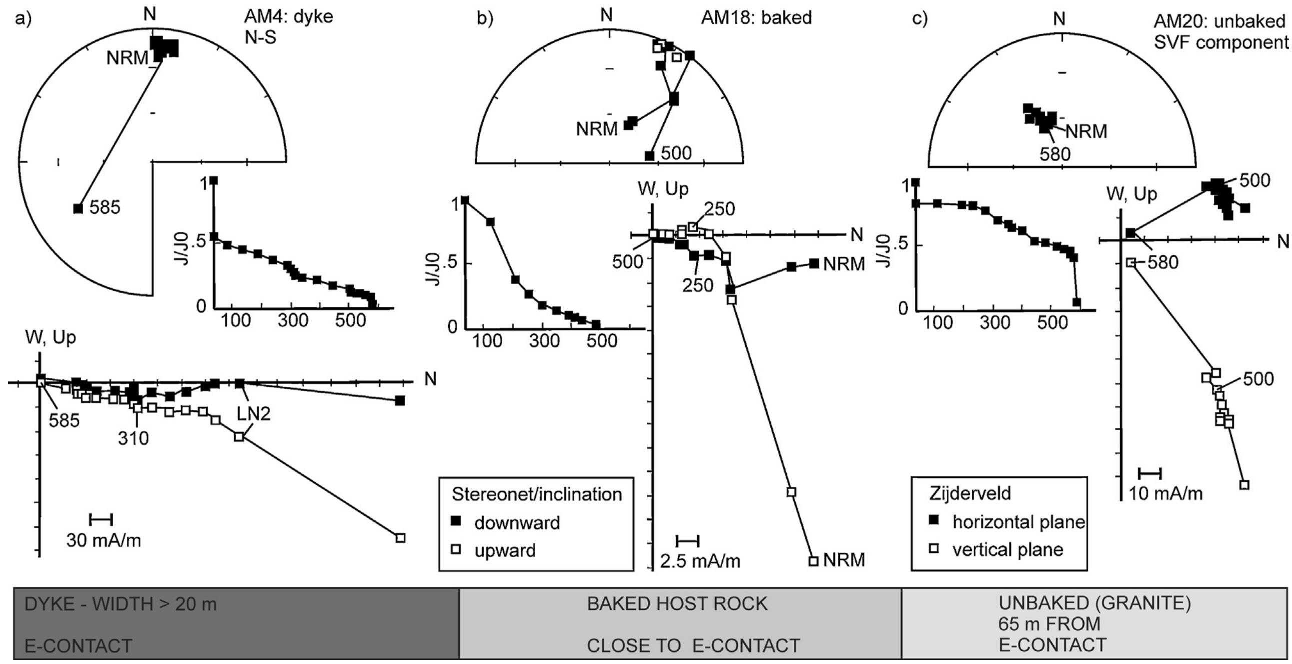


**Fig. 9.** Positive baked contact test for samples from the Satakunta N–S trending dyke (AM), and its baked and unbaked granitic host rock. (a) Dyke sample right at the E-contact, (b) baked host granite from E-contact, and (c) unbaked granite 65 m from contact.

dykes contain more radiogenic Pb (range in $^{206}Pb/^{204}Pb$ ratios from 16.795 to 20.927) than combined Satakunta N–S and NE–SW trending dykes (range in $^{206}Pb/^{204}Pb$ ratios from 16.608 to 18.002), suggesting different magma sources for these groups (Table 5).

## 5. Discussion

### 5.1. Quality of paleomagnetic poles from the Satakunta dykes

Half of the sampled Satakunta dykes show the shallow up- and/or downward pointing P-component, with both normal and reversed directions. The P-component was isolated in the E–W, N–S and NE–SW trending dykes with overlapping $\alpha_{95}$ error cones (Table 2; Fig. 10). The dyke swarms trending N–S and E–W show both normal and reversed directions, but they fail the positive reversal test (McFadden and McElhinney, 1990). Such non-antipodal directions are commonly observed in paleomagnetic records. Several possible hypotheses have been put forward to explain these records, including (1) the insufficient number of sites for the test; (2) the presence of a partially un-removed present-day field magnetization; and (3) changes in magnetic field geometry (e.g. the contribution of an axial octupole, Parés and Van der Voo, 2013). Rock-magnetic experiments show that P is carried by pseudo-single-domain magnetite with unblocking temperatures close to pure magnetite (Table 3; Figs. 14–15), which is not affected by later deformation (Fig. 16).

Geochemical evidence, field observations, and paleomagnetic data (Fig. 18) imply that the E–W trending dykes are older than the N–S and NE–SW trending dykes (Pihlaja, 1987). For example, in Fig. 16, the Nb/Y ratios and Nb concentrations in the N–S and NE–SW trending dykes lie in the same range as those in Åland dykes (1.54–1.57 Ga), and those in E–W trending dykes also sit in the same area as those in Häme and Suomenniemi dykes (1.64–1.67 Ga). Dyke swarms can also be separated based on Pb isotopes. It has

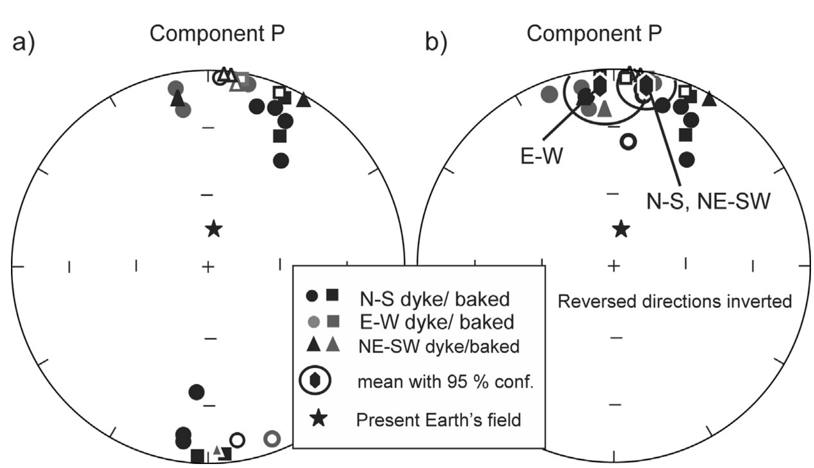


**Fig. 10.** Site mean directions for primary remanent magnetization for Satakunta dykes and their host rocks (see Table 2). (a) Site directions for component P and (b) site directions for component P with antipodal directions inverted. Hexagons represent the mean of both E–W and combined N–S and NE–SW trending dykes. Closed (open) symbols represent downward (upward) directions.

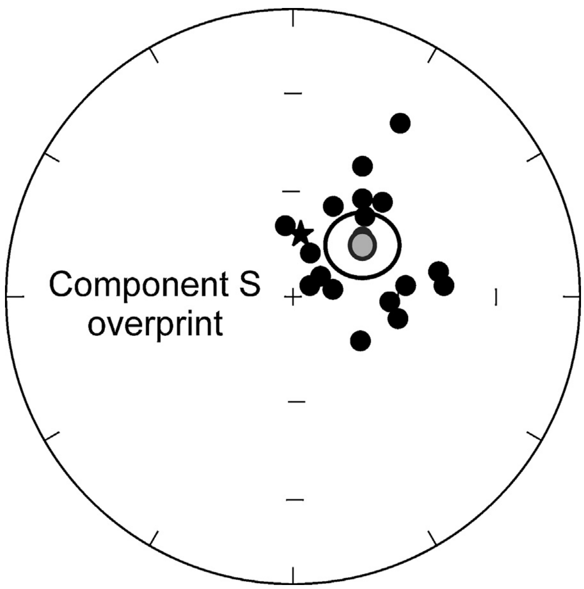


**Fig. 11.** Site mean paleomagnetic directions for interpreted secondary component S. Gray dot represents mean value. Closed (open) symbols represent downward (upward) directions. Black star represents Present Earth Field's direction on the sampling area.

been noted previously (L.J. Pesonen, unpublished data) that Subjotnian (ca. 1.57–1.54 Ga) mafic dykes in Åland Archipelago with reversed magnetization (Kumlinge-Brändö) are older than those with normal magnetization (Föglö-Sottunga). When comparing the position of normal (SK2(N)) and reversed (SK2(R)) poles (see Table 2) from E–W trending Satakunta dykes, pole SK2(R) plots closer to well-defined Svecofennian poles (1.88–1.79 Ga) than pole SK2(N), implying that SK2(R) could be older than the SK2(N). However, since none of these studied E–W trending dykes has been dated, we combine these poles and use that mean in further discussion. Furthermore, the positions of poles SK1(N) and SK1(R) do not indicate any clear age difference. Since only the normal polarity dyke (LS) has been dated, we will use the combined pole SK1 in further discussion. The new paleomagnetic poles are SK2 for E–W (SK2: Plat = 32.6° N, Plong = 205.5° E with $A_{95}$ = 14.3°) and SK1 for combined N–S and NE–SW (SK1: Plat = 29.3° N, Plong = 188.1° E with $A_{95}$ = 6.6°) trending dykes. When comparing the observed between-site dispersion (S) of site-mean paleopoles SK1 and SK2, we obtain "a" values between 11.4° and 15.7° (Table 2), which are consistent with those predicted (13–14°) from the secular variation Model G of Merrill and McElhinny (1983). This indicates that the geomagnetic secular variation has been adequately sampled and that the GAD was operating. The primary nature of both poles is demonstrated by positive baked-contact tests (Fig. 4). Since the error angles of poles SK1 and SK2 are overlapping we cannot truly distinguish their magnetization ages. However, pole SK2 is closer to older paleomagnetic key poles (with Svecofennian age, 1.9–1.8 Ga) than pole SK1 (Fig. 18), probably indicating that the pole SK2 is older than the pole SK1. Unfortunately there are no good quality paleomagnetic data coeval with the Häme dykes (1665–1635 Ma) for comparison. Paleomagnetism of Häme dykes has been reported by Neuvonen (1967), and one dyke belonging to the Häme swarm (Virmaila location) was studied by Salminen and Pesonen (unpublished data). Neuvonen (1967) reported a magnetization direction and pole similar to the secondary component of this study, whereas the Virmaila dyke shows a similar shallow normal polarity direction as the primary component found in this study. These results indicate that earlier methods were inadequate to isolate the primary component (e.g., Neuvonen, 1967 only found the secondary component). The younger Satakunta pole SK1 coincides with the pole of Föglö-Sottunga dykes (1540 ± 12 Ma and 1577 ± 12 Ma) and the error angles overlap with the pole from Bräven-Hälleforsnäs dykes (EW1; 1595 ± 3.5 Ma; 1602 ± 2 Ma, pole 17, Fig. 18), suggesting similar magnetization ages.

The pole SK1 fulfills six quality criteria of paleomagnetic poles (Van der Voo, 1990) providing a new key pole (e.g. Buchan and Halls, 1990; Buchan et al., 2000) for Baltica at 1565 Ma. The only criterion it does not satisfy is a similarity to a younger, but reversed, direction from Baltica in Carboniferous and Permian formations in Sweden and Norway (e.g. Torsvik et al., 1992). However, these areas are more than 500 km to the southwest of our sampling sites, and considering the positive baked contact tests for several dykes it is very unlikely that Carboniferous-Permian geological events generated the remanent magnetization P. Moreover, Pole SK2 satisfies five of Van der Voo's (1990) quality criteria, failing only the aforementioned similarity to younger poles from Baltica, as well as only a half-validated baked contact test, i.e., at one site the baked granite shows similar direction to the dyke, but the unbaked host rock was unstable. However, we have demonstrated that granites (~8 km from this site) carry primary magnetization (~1.88 Ga, Svecofennian).

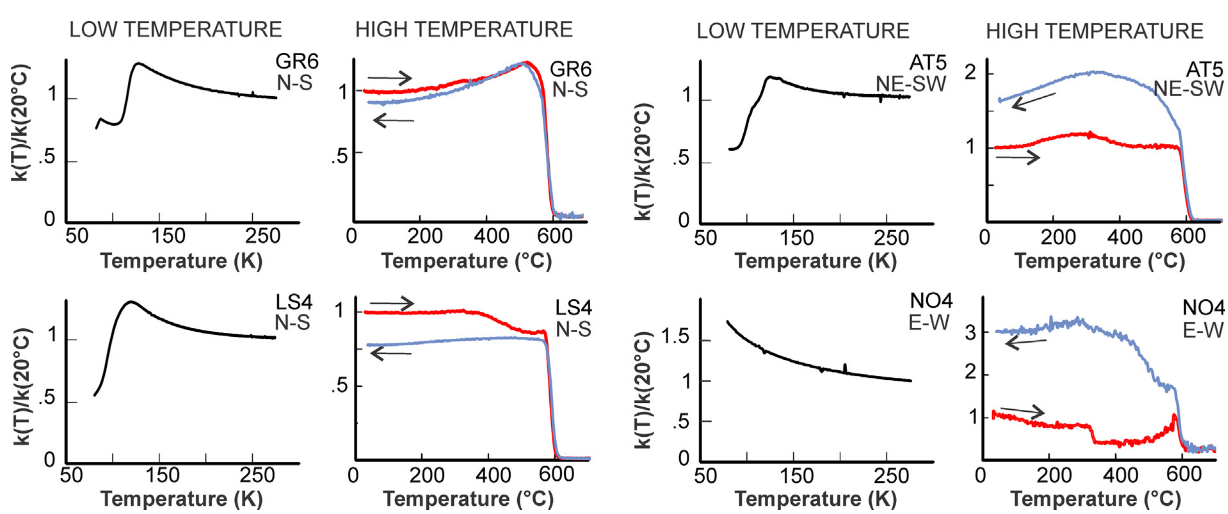


**Fig. 12.** Low and high temperature thermomagnetic curves showing variation in normalized magnetic susceptibility for the Satakunta dyke samples. Curves were corrected for furnace effects.

**Table 3**
Rock magnetic properties for dykes from Satakunta.

| Susceptibility versus temperature | | | | | | Hysteresis | | | | | | | Magnetization versus cold temperature | | | | | | |
|---|---|---|---|---|---|---|---|---|---|---|---|---|---|---|---|---|---|---|---|
| Trend of dykes/sample | $T_{v1}$ (K) | $T_{v2}$ (K) | $T_{C1}$ (°C) | $T_{C2}$ (°C) | Notes | Mr ($Am^2/kg$) | Ms ($Am^2/kg$) | Hc (mT) | Hcr (mT) | Mrs/Mr | Hcr/Hc | $S$ (T) | $RT_{SIRM}$ cooling $t_v$ (K) | $RT_{SIRM}$ heating $t_v$ (K) | $M_{300'}$ (%) | FC $T_v$ (K) | ZFC $T_v$ (K) | Magnetic minerals | Pmag component |
| **N–S** | | | | | | | | | | | | | | | | | | | |
| AM1 | | | | 574 | | | | | | | | | | | | | | mag | $P_N$ |
| GR6 | 126.0 | | | 580 | H | 0.20 | 0.04 | 17.52 | 41.16 | 0.19 | 2.35 | 0.4 | | | | | | PSD mag | $P_R$ |
| HH2 | | | | 580 | H | 0.02 | 0.01 | 66.77 | 84.16 | 0.39 | 1.26 | 0.4 | | | | | | mag | $P_N$ |
| IV7 | 121.0 | | 282 | 582 | H | 0.64 | 0.09 | 9.90 | 3.47 | 0.14 | 0.35 | 0.2 | 116.7 | 124.9 | 68 | 119.4 | 118.5 | PSD mag, mgh? | $P_N$ and PEF/D |
| MA1 | 124.9 | | | 582 | H, S | 2.39 | 0.16 | 5.25 | | 0.07 | | 0.3 | | | | | | SD mag | $P_N$ |
| LS4 | | 116.3 | | 580 | H, c <h | 2.33 | 0.12 | 4.71 | 14.31 | 0.05 | 3.04 | 0.4 | | | | | | PSD mag, mgh? | PEF/$P_N$ |
| **NE–SW** | | | | | | | | | | | | | | | | | | | |
| AT5 | 122.1 | 104.5 | 346 | 582 | | | | | | | | | | | | | | mag, mgh | $P_N$ |
| FB1 | 122.7 | | 342 | 579 | | | | | | | | | | | | | | mgh?, mag | PEF/S |
| FC2 | | 118.8 | | 575 | H, S | 0.08 | 0.01 | 10.35 | 30.18 | 0.13 | 2.92 | 0.6 | 115.9 | 128.5 | 44 | | | PSD mag, mgh | *S* |
| FE3 | 121.6 | 105.1 | 304 | 584 | | | | | | | | | | | | | | PSD mag, mgh | $P_N$ |
| FI4 | 123.2 | | 326 | 584 | | 1.04 | 0.06 | 4.90 | 14.01 | 0.06 | 2.86 | 0.2 | | | | | | PSD mag, mgh/Po? | *S* |
| FK7 | | | | 582 | | 0.18 | 0.02 | 12.62 | 29.84 | 0.13 | 2.37 | 0.3 | | | | | | mag | $P_N$ |
| FS2 | 123.8 | | 446 | 582 | | | | | | | | | | | | | | PSD mag, mgh | *S* |
| FT7 | 128.7 | | 248 | 584 | H | 0.21 | 0.05 | 18.94 | 3.21 | 0.27 | 0.17 | 0.1 | | | | | | PSD mag, mgh | *S* |
| LK4 | 123.8 | | 338 | 578 | H, S | 1.05 | 0.10 | 9.01 | 84.16 | 0.09 | 9.34 | 0.3 | 31.7/115.8 | 33.5/127.7 | 51 | 123.1 | 125.0 | PSD mag, Po, mag | Unstable |
| **E–W** | | | | | | | | | | | | | | | | | | | |
| AO3 | 127.5 | | | 580 | H, S | 0.91 | 0.13 | 12.50 | 22.77 | 0.14 | 1.82 | 0.4 | 117.1 | 127.1 | 52 | | | PSD mag | $P_N$ |
| BR5 | | | | 540 | | | | | | | | | | | | | | mag | Unstable |
| FA2 | 123.8 | | | 580 | S | 1.42 | 0.11 | 6.01 | 13.51 | 0.08 | 2.25 | 0.7 | 124.4 | 127.1 | 48 | | | PSD mag, Po(?) | $P_N$ |
| NI1 | | | 320 | 580 | | | | | | | | | | | | | | mag, mgh | Unstable |
| NO4 | | | 332 | 576 | H | 0.02 | 0.01 | 23.47 | | 0.45 | | 0.2 | | | | | | PSD mag, mgh | $P_N$ |
| NR2 | 124.9 | 108.9 | | 579 | H, S | 2.12 | 0.21 | 9.71 | 12.64 | 0.10 | 1.30 | 0.5 | | | | | | PSD mag, mgh | *S* |
| OJ1 | | | | 581 | | 0.01 | 0.00 | 25.92 | 68.21 | 0.30 | 2.63 | – | | | | | | PSD mag | $P_N$ |
| PR1 | 127.1 | | | 558 | | | | | | | | | | | | | | PSD mag | Unstable |
| SA1 | | | 300 | 537 | | | | | | | | | | | | | | Po/mgh?, mag | *S* |

lat/long – sampling latitude and longitude, Tv1(2) – Verwey transition in Kelvins, $T_{C1/2}$ – Curie points in °C, notes: H – Hopkinson peak; S – shoulder type heating curve; $c < h$ – intensity during cooling is lower than during heating, Mr – saturation remanent magnetization is the maximum magnetization achieved by the specimen in the applied field, Ms – saturation magnetization is the magnetization remaining in the specimen after the field is switched off, Hc – coercive force, Hcr – coercivity of remanence, S – field needed to saturate sample, RTSIRM – 2.5 T SIRM given in room's temperature (300 K), FC – field-cooling in 2.5 T field, ZFC – zero-field-cooling, $M_{300'}$ – memory of the magnetization given in 300 K and then cooled down to 10 K and heated back to 300 K, SD – single-domain; PSD – pseudo-single-domain; MD – multi-domain, mag – magnetite, mgh – maghemite, Po – pyrrhotite, pmag component – obtained component during the paleomagnetic cleaning.

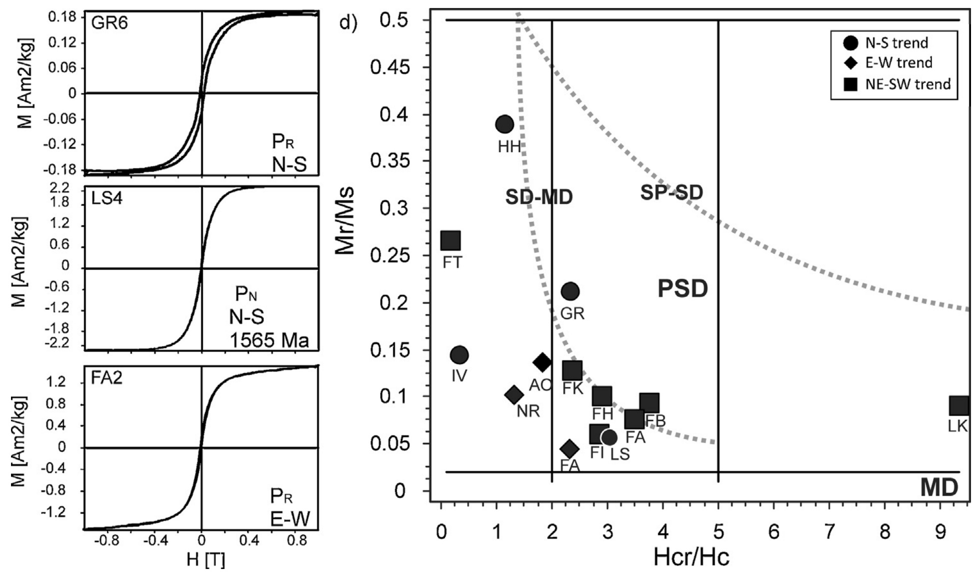


**Fig. 13.** (a)–(c) Examples of hysteresis loops for the selected Satakunta dykes. Trend of the dyke and obtained paleomagnetic component are indicated on lower right corner. (d) Hysteresis data for selected Satakunta dyke samples in Day plot (Day, 1977), which is modified after Dunlop (2002). Mr is saturation remanent magnetization; Ms is saturation magnetization; Hc is coercive force; and Hcr is coercivity of remanence.

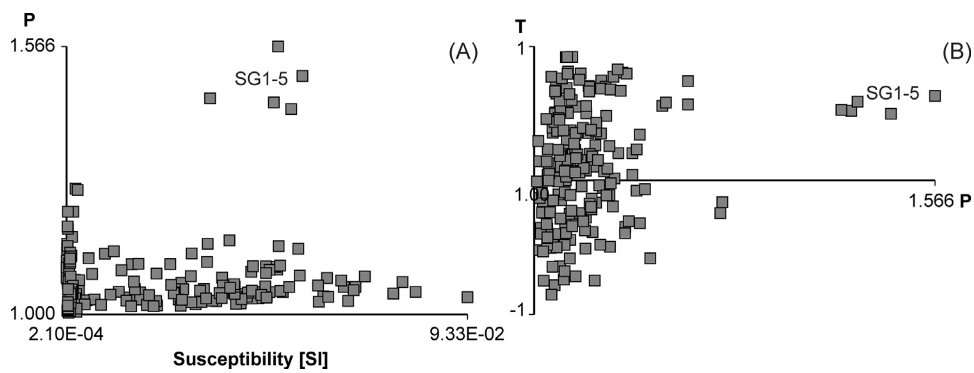


**Fig. 14.** (a) Degree of anisotropy (P) versus bulk susceptibility for all analyzed samples and (b) Jelinek's (1981) shape parameter (*T*) versus degree of anisotropy (*P*) for all analyzed samples.

## *5.2. Other Subjotnian paleomagnetic data for Baltica*

When considering the quality of a paleomagnetic pole it is very important to know both the radiometric age of the rock unit and whether the obtained magnetization is primary. Thus, the numbers (1) and (4) of Van der Voo (1990) quality criteria are considered the most important ones. Many Subjotnian formations, mainly rapakivi granites and associated diabase and quartz-porphyry dykes, have been studied in Fennoscandia (e.g. Neuvonen and Grundström, 1969; Neuvonen, 1970, 1978, 1986; Bylund, 1985; Pesonen et al.,

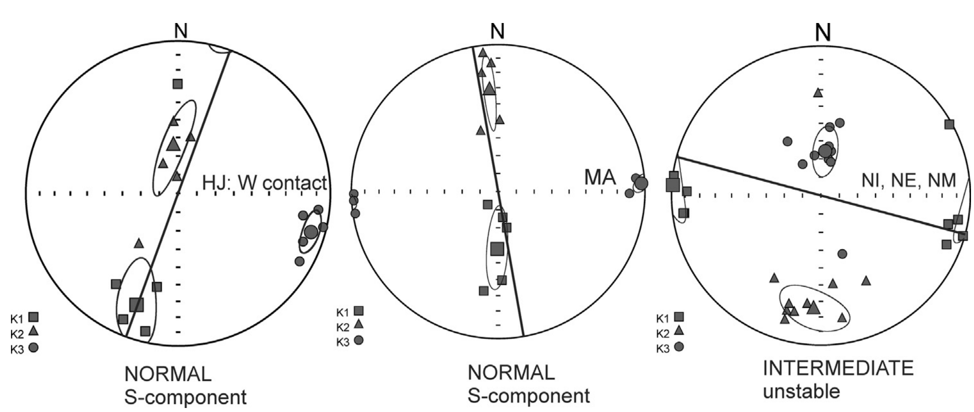


**Fig. 15.** Directions of susceptibility axes on a stereoplots. Examples of normal fabric, where magnetic fabric directions agree with dykes strike, are presented in (a) and (b) and intermediate fabric, where magnetic fabric direction disagree with dykes strike in (c). Symbols: $K_1$ (square) is maximum axis; $K_2$ (triangle) is intermediate axis; and $K_3$ (circle) is minimum axis. Black line represents the orientation (strike) of the dyke. The component obtained in paleomagnetic study is noted below stereoplots.

**Table 4**
Site mean anisotropy of magnetic susceptibility data for Satakunta diabase dykes.

| Trend of dykes/Site | Lat(° N)/long(° E) | Strike | $N$ | $k$ (SI) | $L$ | $F$ | $P$ | $T$ | $K_1$ $D$ (°) | $K_1$ I (°) | $C_{1a}/C_{1b}$ | $K_2$ $D$ (°) | $K_2$ $I$ (°) | $C_{2a}/C_{2b}$ | $K_3$ $D$ (°) | $K_3$ $I$ (°) | $C_{3a}/C_{3b}$ | Fab. | Pmag |
|---|---|---|---|---|---|---|---|---|---|---|---|---|---|---|---|---|---|---|---|
| **N–S** | | | | | | | | | | | | | | | | | | | |
| KA | 62.301/21.379 | 325 | 5 | 0.047 | 1.035 | 1.026 | 1.061 | −0.178 | 315 | 14 | 13/5 | 215 | 34 | 16/11 | 64 | 53 | 16/7 | n | south |
| LS | 62.206/21.429 | 360 | 5 | 0.069 | 1.028 | 1.037 | 1.066 | 0.129 | 348 | 14 | 15/4 | 232 | 61 | 16/2 | 85 | 25 | 7/4 | n | PEF/$P_N$ |
| VA | 62.269/21.434 | 340 | 5 | 0.013 | 1.073 | 1.031 | 1.106 | −0.396 | 118 | 17 | 14/4 | 23 | 16 | 15/2 | 251 | 66 | 6/4 | n | South/S |
| HJ_E cont | 62.059/21.670 | 20 | 5 | 0.038 | 1.017 | 1.021 | 1.038 | 0.148 | 358 | 14 | 28/2 | 88 | 4 | 28/5 | 193 | 75 | 7/3 | im | $P_N$ |
| HJ_W cont | 62.059/21.670 | 20 | 5 | 0.045 | 1.007 | 1.038 | 1.046 | 0.686 | 201 | 23 | 28/9 | 354 | 65 | 28/6 | 106 | 10 | 9/6 | n | $P_N$ |
| IV | 61.542/21.752 | 350 | 5 | 0.027 | 1.014 | 1.025 | 1.040 | 0.198 | 335 | 33 | 20/9 | 94 | 38 | 21/4 | 218 | 36 | 9/5 | n | $P_N$/S |
| PL | 62.279/21.431 | 345 | 5 | 0.042 | 1.024 | 1.037 | 1.062 | 0.191 | 203 | 56 | 55/7 | 346 | 28 | 55/10 | 85 | 17 | 13/9 | n | Unstable |
| GR | 62.240/21.380 | 360 | 5 | 0.040 | 1.063 | 1.064 | 1.130 | 0.031 | 325 | 37 | 12/6 | 193 | 42 | 26/7 | 77 | 27 | 26/11 | n | $P_R$ |
| HH | 61.687/21.594 | 5 | 9 | 0.003 | 1.022 | 1.014 | 1.037 | −0.192 | 66 | 44 | 32/15 | 234 | 45 | 41/18 | 330 | 6 | 35/14 | n | Unstable |
| MA | 61.726/21.609 | 350 | 5 | 0.048 | 1.019 | 1.076 | 1.096 | 0.596 | 181 | 58 | 24/6 | 355 | 32 | 24/3 | 87 | 3 | 7/3 | n | $P_N$/S |
| SG | 62.216/21.399 | 360 | 5 | 0.048 | 1.091 | 1.357 | 1.481 | 0.553 | 108 | 71 | 6/2 | 2 | 6 | 6/3 | 270 | 18 | 4/2 | n | Unstable |
| OV: 3 dykes | 62.154/21.395 | 10 | 8 | 0.036 | 1.025 | 1.025 | 1.050 | 0.107 | 305 | 83 | 37/18 | 167 | 5 | 35/22 | 77 | 5 | 35/32 | n | $P_R$ |
| **NE–SW** | | | | | | | | | | | | | | | | | | | |
| FI;FS | 61.680/21.542 | 40 | 6 | 0.026 | 1.031 | 1.037 | 1.069 | 0.085 | 229 | 17 | 15/9 | 101 | 63 | 13/8 | 326 | 20 | 16/8 | n | *S* |
| FK | 61.680/21.542 | 58 | 9 | 0.002 | 1.029 | 1.014 | 1.043 | −0.336 | 359 | 2 | 57/25 | 268 | 24 | 57/18 | 93 | 66 | 26/17 | n | *S* |
| FE | 61.679/21.545 | 60 | 7 | 0.017 | 1.032 | 1.025 | 1.057 | −0.127 | 229 | 27 | 15/5 | 108 | 46 | 16/10 | 338 | 32 | 14/9 | n | $P_N$/*S* |
| FC | 61.680/21.545 | 60 | 5 | 0.023 | 1.008 | 1.032 | 1.040 | 0.620 | 234 | 72 | 34/6 | 67 | 18 | 34/4 | 336 | 4 | 8/5 | n | *S* |
| FF | 61.687/21.594 | 40 | 5 | 0.009 | 1.096 | 1.050 | 1.153 | −0.355 | 301 | 83 | 27/3 | 131 | 7 | 46/4 | 41 | 1 | 49/11 | im | Unstable |
| FT | 61.680/21.553 | 47 | 8 | 0.029 | 1.020 | 1.027 | 1.048 | 0.134 | 99 | 78 | 66/19 | 286 | 12 | 67/39 | 196 | 2 | 48/21 | im | *S* |
| FD, FH | 61.681/21.546 | 55 | 7 | 0.022 | 1.023 | 1.029 | 1.053 | 0.029 | 88 | 69 | 34/10 | 307 | 17 | 47/21 | 213 | 13 | 44/16 | im | PEF/*S* |
| **E–W** | | | | | | | | | | | | | | | | | | | |
| NI;NE;NM | 61.670/19.843 | 280 | 10 | 0.001 | 1.032 | 1.038 | 1.071 | 0.069 | 274 | 1 | 17/7 | 184 | 24 | 18/11 | 6 | 66 | 14/7 | im | Unstable |
| NO | 61.560/21.820 | 330 | 7 | 0.001 | 1.037 | 1.035 | 1.073 | −0.060 | 335 | 23 | 23/12 | 242 | 6 | 23/13 | 139 | 66 | 18/6 | im | $P_N$ |
| SA | 61.744/21.616 | 270 | 6 | 0.001 | 1.028 | 1.054 | 1.083 | 0.103 | 286 | 7 | 25/20 | 178 | 67 | 57/21 | 19 | 22 | 57/12 | n | *S* |
| NR | 61.560/21.820 | 275 | 9 | 0.068 | 1.017 | 1.026 | 1.044 | 0.155 | 270 | 52 | 47/16 | 7 | 6 | 39/35 | 102 | 38 | 40/31 | im | *S* |
| SL | 62.197/21.441 | 270 | 5 | 0.001 | 1.014 | 1.103 | 1.118 | 0.750 | 89 | 52 | 15/8 | 268 | 38 | 15/7 | 358 | 1 | 11/2 | n | SVF |
| RK | 61.975/22.333 | 270 | 8 | 0.001 | 1.016 | 1.006 | 1.022 | −0.408 | 1 | 64 | 7/6 | 142 | 21 | 48/6 | 238 | 15 | 48/6 | im | *S* |
| FA | 61.679/21.545 | 270 | 7 | 0.047 | 1.017 | 1.024 | 1.041 | 0.031 | 9 | 71 | 64/12 | 253 | 9 | 64/42 | 161 | 17 | 43/21 | n | $P_R$/*S* |
| Mean | | | 166 | 0.025 | 1.026 | 1.035 | 1.062 | | | | | | | | | | | | |

Lat/long – sampling latitude and longitude, $N$ – number of samples, $k$ – bulk mean susceptibility, $L$ – magnetic lineation: $L = K_1/K_2$, $F$ – foliation: $F = K_2/K_3$, $P$ – degree of anisotropy: $P = K_1/K_3$, $T$ – Jelinek's shape parameter (Jelinek, 1981): $T = [2\ln(K_2/K_3)/\ln(K_1/K_3)] - 1$, $K_1$, $K_2$ and $K_3$ – mean AMS eigen vectors, which represent the maximum, intermediate and minimum susceptibility axis, respectively, $C_{1(2,3)a}/C_{1(2,3)b}$ – semi-angles of the major and minor axes of 95% confidence ellipse, Fab. – observed fabric: n, normal; im, intermediate, Pmag – obtained component during paleomagnetic cleaning.

**Table 5**
Whole rock Pb isotopic composition of Satakunta and Sipoo Subjotnian dyke samples.

| Sample | Trend | Nb (ppm) | Y (ppm) | Nb/Y | $^{206}Pb/^{204}Pb$ | Error 2$\sigma$ | $^{207}Pb/^{204}Pb$ | Error 2$\sigma$ |
|---|---|---|---|---|---|---|---|---|
| **Satakunta** | | | | | | | | |
| AM8 | N–S | 6.42541 | 16.16315 | 0.397534 | 17.43249 | 0.00179 | 15.51951 | 0.00169 |
| AM15 | N–S | 14.53996 | 40.54537 | 0.35861 | 17.381173 | 0.00272 | 15.50314 | 0.00245 |
| GR2 | N–S | 13.6871 | 34.78138 | 0.393518 | 16.842105 | 0.00175 | 15.44417 | 0.00158 |
| GR6 | N–S | 14.74729 | 38.06752 | 0.387398 | 17.117234 | 0.00192 | 15.47661 | 0.00186 |
| HJ3 | N–S | 11.55158 | 36.19871 | 0.319116 | 16.640045 | 0.00280 | 15.4201 | 0.00249 |
| HJ8 | N–S | 12.13263 | 34.83948 | 0.348244 | 16.607516 | 0.00429 | 15.41815 | 0.00278 |
| LS1 | N–S | 30.89705 | 86.18967 | 0.358477 | 16.772165 | 0.00152 | 15.44297 | 0.00160 |
| OV2 | N–S | 11.02472 | 34.26518 | 0.321747 | 16.901321 | 0.00209 | 15.44494 | 0.00182 |
| VA2 | N–S | 24.90825 | 53.07072 | 0.469341 | 16.658305 | 0.00125 | 15.43039 | 0.00115 |
| AT3 | NE–SW | 34.60376 | 82.89722 | 0.41743 | 18.001753 | 0.00172 | 15.57205 | 0.00154 |
| FB6 | NE–SW | 22.14079 | 45.46294 | 0.487007 | 16.876835 | 0.00182 | 15.44471 | 0.00178 |
| FK4 | NE–SW | 18.51105 | 44.30201 | 0.417838 | 16.905494 | 0.00157 | 15.44861 | 0.00154 |
| FK14 | NE–SW | 20.34388 | 41.10707 | 0.4949 | 16.724737 | 0.00178 | 15.42863 | 0.00178 |
| AO3 | E–W | 5.845264 | 13.00106 | 0.449599 | 17.232005 | 0.00251 | 15.48936 | 0.00221 |
| FA2 | E–W | 23.62465 | 47.88119 | 0.493401 | 16.795154 | 0.00177 | 15.43775 | 0.00171 |
| FA8 | E–W | 22.16113 | 42.22913 | 0.524783 | 16.879112 | 0.00197 | 15.44857 | 0.00181 |
| SL2 | E–W | 24.98991 | 29.33798 | 0.851794 | 18.357468 | 0.00318 | 15.61867 | 0.00277 |
| **Sipoo diabase** | | | | | | | | |
| SC1 | E–W | 44.64954 | 44.41855 | 1.0052 | 17.587254 | 0.00224 | 15.52636 | 0.00210 |
| SC6 | E–W | 48.12103 | 57.9343 | 0.830614 | 17.708768 | 0.00210 | 15.54301 | 0.00184 |
| SG4 | NW–SE | 47.6181 | 50.99451 | 0.933789 | 17.808986 | 0.00199 | 15.5479 | 0.00177 |
| SG3 | NW–SE | 49.32342 | 47.21222 | 1.044717 | 17.473038 | 0.00182 | 15.51572 | 0.00166 |
| SF3 | NNE–SSW | 53.31565 | 53.45127 | 0.997463 | 18.023488 | 0.00200 | 15.57932 | 0.00180 |
| **Sipoo quartz porphyry** | | | | | | | | |
| PN4 | NW–SE | 50.96362 | 123.0377 | 0.414212 | 20.438554 | 0.00127 | 15.83424 | 0.00117 |
| PN8 | NW–SE | 53.18633 | 114.9975 | 0.4625 | 20.927274 | 0.00162 | 15.87693 | 0.00146 |
| PV8 | NW–SE | 71.10264 | 137.0688 | 0.518737 | 19.455662 | 0.00155 | 15.66483 | 0.00135 |
| PV9 | NW–SE | 70.42737 | 126.7407 | 0.555681 | 19.130062 | 0.00140 | 15.6659 | 0.00131 |
| SA2 | NW–SE | 35.41246 | 63.67719 | 0.556125 | 17.272917 | 0.00121 | 15.51173 | 0.00119 |

1987, 1991; Pesonen, 1987; Bylund and Elming, 1992; Mertanen and Pesonen, 1995; Mertanen et al., 2008). These Subjotnian data are scattered, and $A_{95}$ error angles of many of these poles are overlapping (Fig. 18b, Table 6). Some of them seem to be overprinted by later geological processes, and others do not have good age constraints. More importantly, some of them do not have positive baked contact test results. Only four Subjotnian poles for Baltica samples meet the two most important criteria (but may have problems in others): (1) Nordingrå granite, 1578 ± 19 Ma (Piper, 1980); (2) Kumlinge-Brändö dykes, 1571 ± 9 Ma (Pesonen and Neuvonen, 1981); (3) Satakunta SK1, 1565 Ma; and (4) Föglö-Sottunga dykes in Åland, 1540 ± 12 Ma and 1577 ± 12 Ma (Pesonen and Neuvonen, 1981). The pole from Nordingrå granite (1578 ± 19 Ma) is somewhat offset from the other ca. 1580 Ma poles (Fig. 18), which may arise from the fact that there is no control over the possible tilting of the granite at the time of remanence acquisition (Piper, 1980).

A closer look at Baltica's Subjotnian paleomagnetic data reveal that large scatter may be due to several reasons. As an explanation we favor unrecognized overprinting and/or unrecognized tilting of granites. An additional explanation, especially for the reversed polarity data, could be the simultaneous reversing of the Earth's magnetic field when the dykes acquired their magnetization. Scatter may arise also from individual plate motion (perhaps Baltica alone, or perhaps within the Nuna supercontinent; Zhang et al., 2012) or true polar wander at 1.6–1.5 Ga. Full understanding of these issues awaits further data collection and analysis.

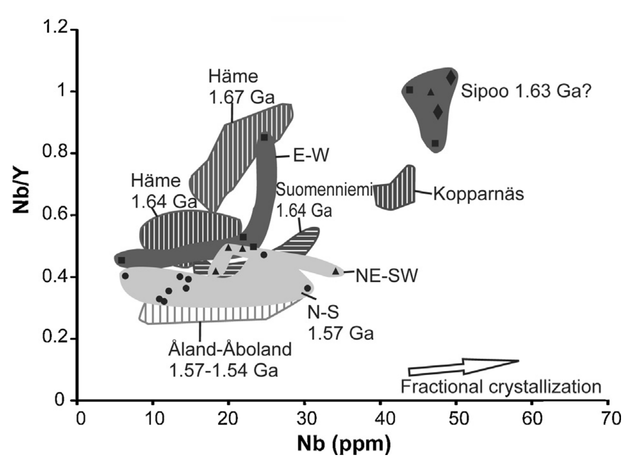


**Fig. 16.** Variation of Nb/Y versus Nb for the Satakunta and Sipoo (1633 Ma) Subjotnian dykes (Table 5). Compositional fields for other Subjotnian (Häme, Suomenniemi, Åland-Åboland, Kopparnäs) are shown for comparison (data from Luttinen and Kosunen, 2006). Fields of older (1.67 Ga) and younger (1.64 Ga) Häme dykes are shown separately.

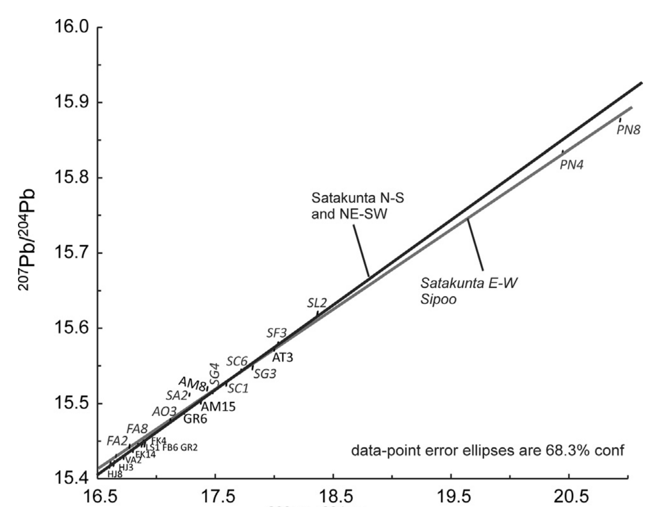


**Fig. 17.** Pb–Pb diagram showing the isotope ratios for measured Satakunta and Sipoo Subjotnian diabase dykes (Table 5).

**Table 6**
Selected paleomagnetic poles for Baltica and Laurentia.

| Code | Pole/formation | Plat (° N) | Plong (° E) | $A_{95}$(°) | Euler pole (° N/° E/angle°) | RPlat (° N) | RPlong (° E) | Age (Ma) | 1 | 2 | 3 | 4 | 5 | 6 | Σ | Reference |
|---|---|---|---|---|---|---|---|---|---|---|---|---|---|---|---|---|
| **Baltica-Fennoscandia** | | | | | | | | | | | | | | | | |
| 1 | Konchozero sill | −14 | 282 | 10 | | | | 1974 ± 27 | 1 | 0 | 1 | 1 | 1 | 0 | 4 | Pisarevsky and Sokolov (1999) |
| 2 | Mean Svecofennian 1 | 41 | 233 | 5 | | | | 1881 | 1 | 1 | 1 | 0 | 0 | 0 | 3 | Pesonen et al. (2003) |
| 3 | Mean Svecofennian 2 | 48 | 225 | 3 | | | | 1840 | 1 | 0 | 1 | 0 | 0 | 1 | 3 | Pesonen et al. (2003) |
| 4 | Shoksha sandstones | 40 | 221 | 4 | 47/1.5/49.5[a] | 13 | 266 | 1790–1770 | 0 | 1 | 1 | 1 | 1 | 1 | 5 | Pisarevsky and Sokolov (2001) |
| 5 | Hoting gabbro[c] | 43 | 233 | 11 | | | | 1786 ± 10 | 1 | 1 | 1 | 1 | 0 | 0 | 4 | Elming et al. (2009) |
| 6 | MEAN Ropruchey sill | 39 | 217 | 7 | 47/1.5/49.5[a] | 10 | 273 | 1770 ± 12 | 1 | 0 | 1 | 0 | 1 | 0 | 3 | Pisarevsky and Sokolov (2001) |
| 7 | Sipoo diabase | 32 | 184 | 31 | | | | 1633? | 1 | 0 | 1 | 0 | 1 | 0 | 3 | Mertanen and Pesonen (1995) |
| 8 | Sipoo quartz porphyry | 26 | 180 | 7 | 47/1.5/49.5[a] | 11 | 233 | 1633 ± 10 | 1 | 1 | 1 | 0 | 1 | 0 | 4 | Mertanen and Pesonen (1995) |
| 9 | SE Quartz porphyry dykes | 30 | 175 | 9 | | | | 1617 ± 2, 1639 ± 9, 1638 ± 53 | 1 | 0 | 1 | 0 | 1 | 0 | 3 | Neuvonen (1986) |
| 10 | Hoting basic dykes[c] | 21.9 | 146.7 | 13.7 | | | | 1614 ± 24 (?) | 1 | 0 | 1 | 1 | 1 | 0 | 4 | Elming et al. (2009) |
| 11 | Nordingrå gabbro anorthosite | 36.9 | 138.1 | 4.7 | | | | 1578 ± 19 | 1 | 1 | 1 | 0 | 0 | 1 | 4 | Piper (1980) |
| 12 | Nordingrå granite | 32.4 | 149 | 10.5 | | | | 1578 ± 19 | 1 | 0 | 1 | 1 | 0 | 1 | 5 | Piper (1980) |
| 13 | Kumlinge-Brändö dykes[c] | 12 | 182 | 7 | | | | 1571 ± 9, 1576 ± 13 | 1 | 1 | 0 | 1 | 1 | 0 | 4 | Pesonen and Neuvonen (1981) |
| 14 | Satakunta N–S and NE–SW: SK1[c] | 29 | 188 | 7 | 47/1.5/49.5[a] | 12 | 236 | 1565 | 1 | 1 | 1 | 1 | 1 | 1 | 6 | This work |
| 15 | Satakunta E–W: SK2 | 33 | 206 | 14 | 47/1.5/49.5[a] | 8 | 251 | – | 0 | 1 | 1 | 1 | 1 | 1 | 5 | This work |
| 16 | Mean Satakunta combined | 30 | 192 | 6 | 47/1.5/49.5[a] | 11 | 240 | | 1 | 1 | 1 | 1 | 1 | 1 | 6 | This work |
| 17 | Bräven-Hälleforsnäs EW1 | 28 | 197 | 6 | | | | 1595 ± 3.5, 1602 ± 2 | 1 | 0 | 1 | 0 | 1 | 0 | 3 | Bylund (1985) |
| 18 | Bräven-Hälleforsnäs EW2[d] | 62 | 176 | 11 | | | | 1510–1560 | 1 | 0 | 1 | 0 | 1 | 0 | 3 | Bylund (1985) |
| 19 | Föglö-Sottunga dykes[c] | 28 | 188 | 9 | 47/1.5/49.5[a] | 11 | 236 | 1540 ± 12, 1577 ± 12 | 1 | 1 | 0 | 1 | 1 | 0 | 4 | Pesonen and Neuvonen (1981) |
| 20 | Ragunda dykes 2[d] | 64.1 | 154.5 | 24.7 | | | | 1505 ± 12, 1514 ± 5 | 1 | 0 | 1 | 0 | 1 | 1 | 4 | Piper (1979) |
| 21 | Post-Ragunda dykes 1 | 14.6 | 194.4 | 11.1 | | | | 1350–1520 | 0 | 1 | 1 | 0 | 1 | 1 | 4 | Piper (1979) |
| 22 | Ragunda frm | 51.6 | 166.6 | 7.1 | | | | 1514 ± 5 | 1 | 1 | 1 | 0 | 0 | 1 | 4 | Piper (1979) |
| 23 | Ragunda rapakivi | 49.1 | 171 | 20.3 | | | | 1503 ± 12, 1513 ± 9 | 1 | 0 | 1 | 0 | 0 | 0 | 2 | Piper (1979) |
| 24 | Rödö dykes | 41.6 | 201.7 | 10 | | | | – | 0 | 1 | 1 | 1 | 1 | 0 | 4 | Moakhar and Elming (2000) |
| 25 | Rödö granites[d] | 6.2 | 175 | 5 | | | | 1513 | 0 | 1 | 1 | 0 | 0 | 0 | 2 | Moakhar and Elming (2000) |
| 26 | Salmi formation | 6 | 200 | 11 | | | | 1460 | 1 | 1 | 1 | 0 | 1 | 0 | 4 | Shcherbakova et al. (2006) |
| 27 | Tuna dykes | 21 | 171 | 10 | | | | 1474 ± 4 | 1 | 1 | 1 | 0 | 1 | 0 | 4 | Piper (1992) |
| 28 | Valaam monzodiorite | 14 | 166 | 2 | | | | 1458 ± 4 | 1 | 1 | 1 | 0 | 1 | 0 | 4 | Salminen and Pesonen (2007) |
| 29 | Lake Ladoga mafic rocks[c] | 15 | 177 | 6 | 47/1.5/49.5[a] | 5 | 220 | 1452 ± 12 | 1 | 1 | 1 | 1 | 1 | 1 | 6 | Lubnina et al. (2010) |
| 30 | Mean post-Jotnian intrusions[c] | 4 | 158 | 4 | 47/1.5/49.5[a] | 6 | 198 | 1265 | 1 | 1 | 1 | 1 | 1 | 0 | 5 | Pesonen et al. (2003) |
| **Laurentia** | | | | | | | | | | | | | | | | |
| Cle | Cleaver dykes[c] | 19 | 277 | 6 | | | | 1740 +5/−4 | 1 | 1 | 1 | 1 | 1 | 0 | 5 | Irving et al. (2004) |
| Dub | Dubawnt group[c] | 7 | 277 | 8 | | | | 1785 ± 4 | 1 | 1 | 1 | 1 | 1 | 1 | 6 | Park et al. (1973) |
| Mel | Melville Bugt dyke swarm | 5 | 274 | 9 | 67.5/241.5/−13.8[b] | 2 | 262 | 1622 ± 3, 1635 ± 3 | 1 | 1 | 1 | 0 | 1 | 1 | 5 | Halls et al. (2011) |
| WCD | Western Channel diabase[c] | 9 | 245 | 7 | | | | 1592 ± 3, 1590 ± 4 | 1 | 1 | 1 | 1 | 1 | 0 | 5 | Irving et al. (1972), Hamilton and Buchan (2010) |
| | Michikamau intrusion[c] | −2 | 218 | 5 | | | | 1460 ± 5 | 1 | 1 | 1 | 1 | 0 | 1 | 5 | Emslie et al. (1976) |
| | St. Francois Mnt acidic rocks[c] | −13 | 219 | 6 | | | | 1476 ± 16 | 1 | 1 | 1 | 1 | 1 | 0 | 5 | Meert and Stuckey (2002) |
| Mean | Mean | −7 | 218 | 6 | | | | 1468 | | | | | | | | Interpolated |
| Mac | MacKenzie dykes grand mean[c] | 4 | 190 | 5 | | | | 1267 + 7/−3 | 1 | 1 | 1 | 1 | 1 | 0 | 5 | Buchan and Halls (1990) |

Code – code in Fig. 19; Plat – pole latitude; Plong – pole longitude; $A_{95}$ – Fisher statistics parameter. RPlat(RPlong) – rotated pole latitude(longitude).

[a] Used rotation of Evans and Pisarevsky (2008) for Baltica to Laurentian reference frame.

[b] Used rotation of Roest and Sirvastava (1989) for Greenland to Laurentian reference frame.

[c] Primary magnetization demonstrated by baked contact test from the dated rock units.

[d] Suspected overprinted magnetic direction.

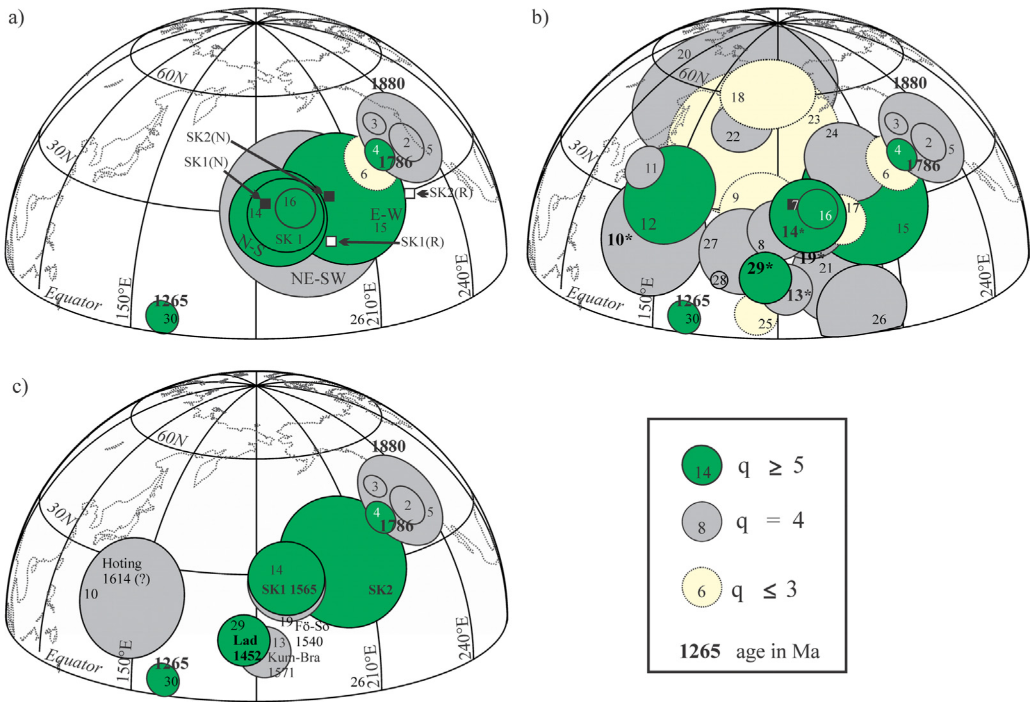

**Fig. 18.** (a) Satakunta paleomagnetic poles from dykes by different trends with relevant Precambrian poles for Baltica. Normal (black, N) and reversed (white, R) data for SK1 and SK2 poles are presented as squares without error bars. See coding in Tables 2 and 6, (b) poles from this study with other Subjotnian and relevant Precambrian paleomagnetic poles of Baltica. We have marked with * the most reliable Subjotnian poles (see Section 5.2), and (c) selected poles of Baltica with $q \geq 4$. See numbering in Table 6.

### *5.3. Long-lasting NENA configuration within supercontinent NUNA*

Based on a tight cratonic fit, concordance with basement geology, correlations of geochronology, and matching of recent paleomagnetic poles, some authors favor the long-lasting (1.8–1.2 Ga) configuration of Baltica and Laurentia in the NENA (North Europe-North America) configuration whereby eastern Greenland is juxtaposed with the Timanide-Uralide margin of Baltica (e.g. Gower et al., 1990; Buchan et al., 2000; Salminen and Pesonen, 2007; Evans and Pisarevsky, 2008; Pisarevsky and Bylund, 2010) forming the core of the supercontinent Nuna (see

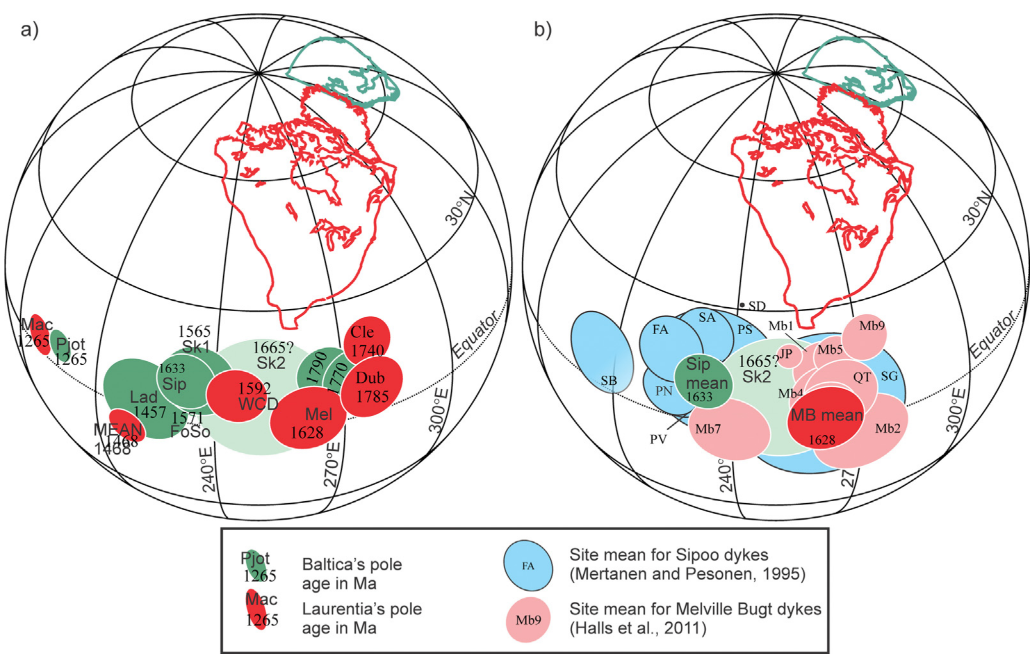

**Fig. 19.** Testing the NENA fit. (a) High quality poles of Laurentia and Baltica rotated to NENA configuration. Used poles are listed in Table 6, (b) virtual geomagnetic poles for Melville Bugt dykes, Greenland (normal polarity is used; Halls et al., 2011) and for Sipoo dykes, Finland (Mertanen and Pesonen, 1995). Additionally SK2 pole of this study is plotted. Baltica and its poles are rotated to reference frame of Laurentia by Euler pole: Plat = 47°, Plong = 1.5°, angle = 49° (Evans and Pisarevsky, 2008). Poles from Greenland are rotated to reference frame of Laurentia by Euler pole: Plat = 67.5°, Plong = 241.5°, angle = –13.8° (Roest and Sirvastava, 1989).

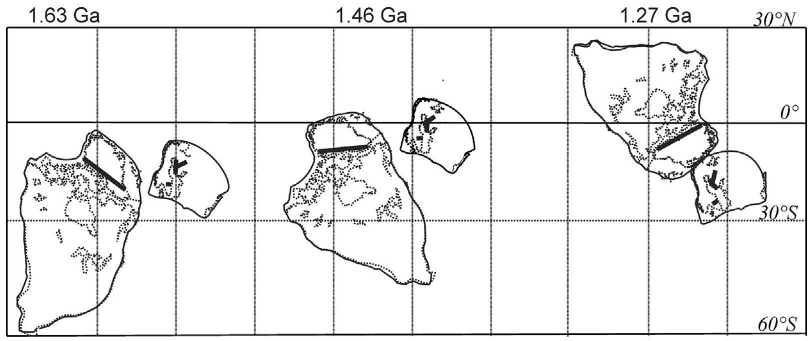


**Fig. 20.** Reconstructions of Baltica (B) and Laurentia (L) at 1.63 Ga, and 1.46 Ga suggested by Halls et al. (2011) that differ from proposed long lasting NENA fit (Gower et al., 1990; Patchett et al., 1978; Piper, 1980; Pesonen et al., 2003; Salminen and Pesonen, 2007; Evans and Pisarevsky, 2008; Pisarevsky and Bylund, 2010; Pesonen et al., 2012) and reconstruction at 1.27 Ga (Pesonen et al., 2003). For 1.63 Ga – B: reinterpreted data from Sipoo porphyry dykes, Finland (Halls et al., 2011). L: location of Laurentia based on an adjustment of the Melville Bugt (Greenland) pole position that lies within its 95% confidence circle (Halls et al., 2011). For this reconstruction Melville Bugt pole from Greenland was at first rotated to reference frame of Laurentia (see Table 6). In this reconstruction the used polarity for Melville Bugt and Sipoo are different. For 1.46 Ga – B: combined Lake Ladoga area and Valaam sill (1452 ± 12 Ma) pole, Russia (Salminen and Pesonen, 2007; Lubnina et al., 2010). L: mean pole 1460 Ma (calculated in Salminen and Pesonen, 2007). For 1.265 Ga – B: mean pole from Postjotnian mafic dykes (1.265 Ga), Finland (Pesonen et al., 2003). L – MacKenzie dykes (1.265 Ga), Canada (Buchan and Halls, 1990) in NENA fit. Black line in Greenland (Baltica) cartoon indicates Melville Bugt dykes (Häme, Satakunta, and Bräven-Hälleforsnäs dykes related to rapakivi magmatism).

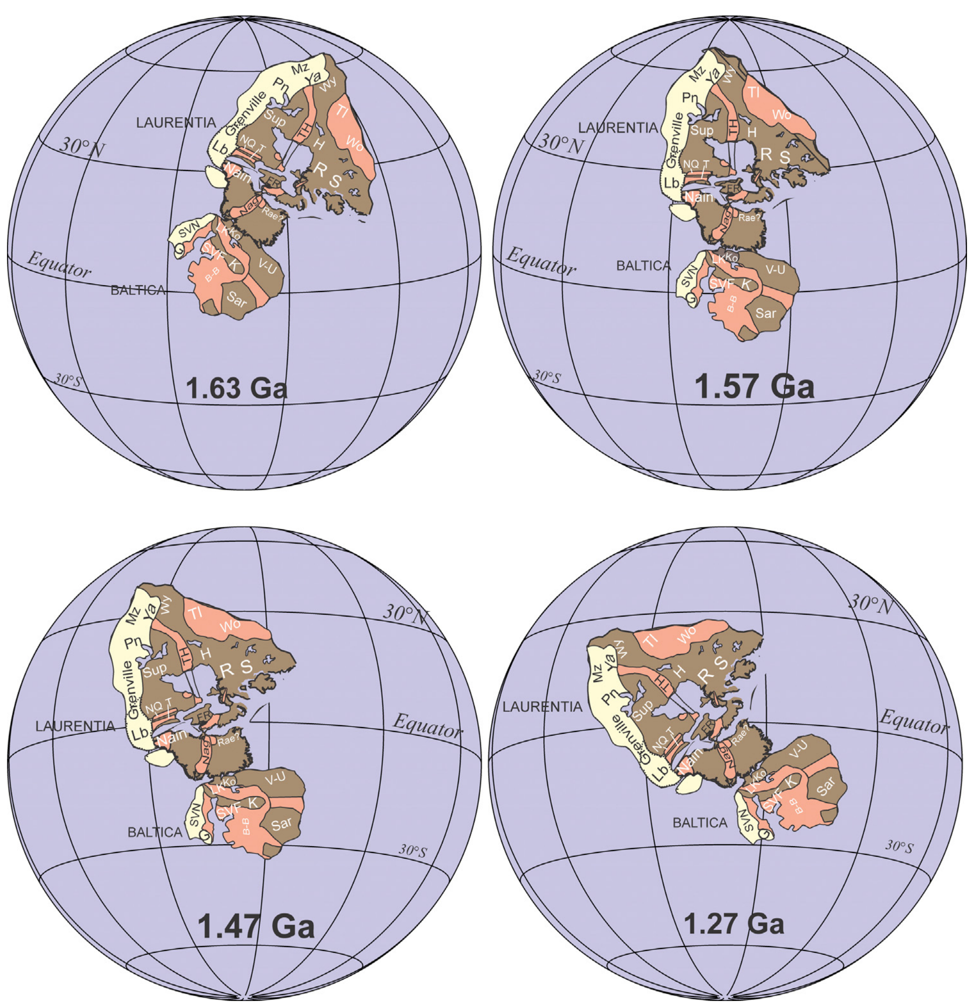


**Fig. 21.** Reconstruction of Baltica and Lauretina between 1.63 Ga and 1.27 Ga forming the core of NENA. Data are listed in Table 6. Archean cratonic areas: Baltica (Ko – Kola; K – Karelia; V-U – Volgo-Uralia; Sar – Sarmatia); Laurentia: (S – Slave, Sup – Superior, H – Hearne; R – Rae; Wy – Wyoming; Nain in Greenland). Proterozoic: Baltica (SVF – Svecofennian domain; LK – Lapland-Kola; G – Gothian; B-B – Baltic-Belarus; SVN – Sveconorwegian); and Laurentia (Pn – Panokean; Mz – Mazatzal; Ya – Yavapai; TH – Trans-Hudson; Tl – Taltson; Wo – Wopmay; NQ – New Quebeck; T – Tornget, FR Foxe-Rinklan; Lb – Labradorian; Nag – in Greenland).

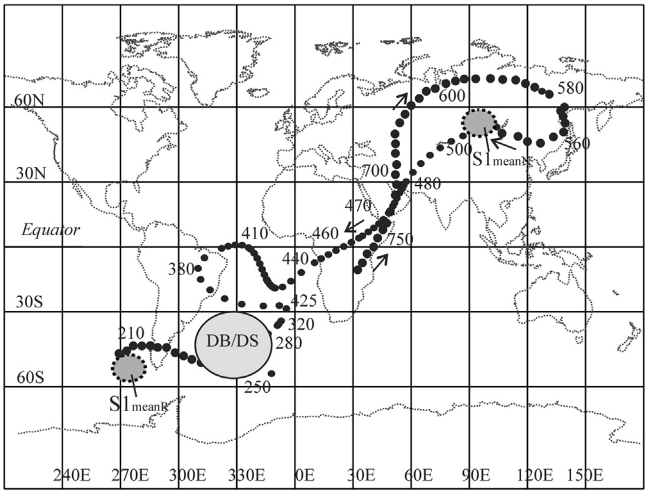


**Fig. 22.** Secondary pole from Satakunta dykes plotted on the Paleozoic apparent polar wander path of the Fennoscandian shield (Torsvik et al., 1996). Secondary DB/DS pole from Olkiluoto (Mertanen et al., 2008). Numbers indicate years in Ma.

also Hoffman, 1989, 1996; Åhäll and Connelly, 1998; Meert, 2002; Rogers and Santosh, 2002; Zhao et al., 2004; Condie, 2004; Pesonen et al., 2012). Paleomagnetic poles can be used to test the duration of a particular continental configuration by rotating coeval poles to the appropriate configuration (e.g. Evans and Pisarevsky, 2008). If the poles overlap there is paleomagnetic evidence consistent with that configuration for the proposed time interval. We have rotated selected key paleomagnetic poles of Baltica to the present reference frame of North America in the NENA configuration, using Euler parameters of Elat = 47.5°, Elong = 1.5°, angle = 49° (Evans and Pisarevsky, 2008; Table 6). In this reconstruction the combined mean pole of Satakunta (1565 Ma) overlaps with the 1592 ± 3 Ma Western Channel Diabase (WCD) pole (Fig. 19a) indicating that the NENA configuration is permissible based on paleomagnetic data. NENA is also valid at 1.75 Ga, at 1.46 Ga and at 1.27 Ga (Fig. 19). In the NENA fit, Archean to Paleoproterozoic formations are continuous from North America through Greenland to northern Baltica. For example, these fits allow correlations of subduction-related magmatism at around 1.7 Ga, stretching from the 1.8–1.7 Ga Yavapai and 1.7–1.6 Ga Mazatzal provinces in southwestern Laurentia, through the 1.7–1.6 Ga Labradorian province of eastern Laurentia, to the 1.7–1.5 Ga Gothian province of southwestern Baltica. Likewise, the trends of coeval 1.27 Ga MacKenzie dykes in Laurentia and Post-Jotnian dykes in Baltica become contiguous in these reconstructions (see also Pesonen et al., 2003; Elming and Mattsson, 2001). The well-known 1.27 Ga reconstruction avoids polarity ambiguity since the data from mafic dykes of both Laurentia and Baltica are of single polarity (Pesonen et al., 2003).

Despite the geological and paleomagnetic evidence for the joint history between 1.8 Ga and 1.27 Ga, recent mean paleomagnetic data from Greenland appear to argue against the NENA configuration. In detail, the paleomagnetic pole of Melville Bugt dykes (Greenland; 1622 ± 3 Ma, 1635 ± 3 Ma; Halls et al., 2011) does not overlap with the coeval pole of Sipoo dykes (Finland; 1633 Ma; Mertanen and Pesonen, 1995) in the NENA reconstruction (Fig. 19a), but it overlaps with the Satakunta SK2 pole (E–W dykes). Moreover, if the Satakunta SK2 pole from this study represents that having the same age as the Häme dykes (1665–1635 Ma; Vaasjoki et al., 1991), then it supports the NENA fit at 1.63 Ga (Fig. 19). However, the individual site-mean data from both Melville Bugt and Sipoo dykes show a large scatter between the virtual geomagnetic poles of both continents, which does not exclude the possibility that continents were together at 1.63 Ga (Fig. 19b).

In producing paleomagnetic and geochronological data from Melville Bugt dykes, Halls et al. (2011) proposed a continental configuration whereby Laurentia and Baltica are juxtaposed so that the southern end of the Melville Bugt dyke swarm can be projected toward the Fennoscandian rapakivi province (Fig. 20). Based on the proximity and geochemical data, Halls et al. (2011) suggest that Melville Bugt dykes in Greenland are fed by the source below the continental crust underneath Fennoscandian rapakivi province, which is also the source for the Fennoscandian rapakivi-related magmas. However, there are a few concerns with their reconstruction. First, the use of different polarity options for coeval paleopoles from Laurentia and for a modified pole of Baltica (Sipoo dykes, Finland – 1633 Ma) could be problematic of matching the well-known 1.26 Ga reconstruction that has no polarity ambiguity (Pesonen et al., 2003). Second, the Subjotnian dykes in Fennoscandia do not support the same magma source for Melville Bugt and Fennoscandian dykes for four reasons: (1) the variations in major elements and REE geochemical compositions of Subjotnian dykes in Finland (such as Häme and Åland archipelago dykes) are large and outside the geochemical range of Melville Bugt dykes (Luttinen and Kosunen, 2006); (2) recent geochemical data indicate different sources for Subjotnian dykes within Finland (Salminen, unpublished data); (3) the widths of the dykes in Fennoscandia are so narrow that they could not have been able to feed the huge Greenland dykes; and (4) the age distribution of dykes in Fennoscandia do not support the same magma source with Greenland dykes. The age of the Sipoo dykes (Southeast Finland) agrees with Melville Bugt dykes, but other Subjotnian dykes in between these intrusions, in southwest Finland and in Sweden, are younger. Consequently, we propose that the NENA fit, where Baltica occupied low latitudes, shown in Fig. 21, was valid also at 1.63–1.56 Ga, and that it formed the core of Nuna during 1.8–1.2 Ga. The Mesoproterozoic 1.5–1.3 Ga red-bed sedimentation (for example the Satakunta sandstone) also supports this low-latitude location of Baltica in Subjotnian times (Rämö et al., 2005; Klein et al., in this volume).

### *5.4. Secondary magnetization, Pole S*

Fifteen sites show a secondary component S as a lower unblocking temperature overprint (Table 2; Fig. 11). This component S has pole: Plat = 53.3° N, Plong = 103.9° E, $A_{95}$ = 13.2° (Table 2) and is obtained mainly from the weathered NE–SW trending dykes and in the samples taken from the coarser grained interior of the dykes. It has been suggested that NE–SW and NW–SE trending brittle fractures, which formed during the NW–SE directed stress field that caused normal faulting on Svecofennian domain, have been most vulnerable to later reactivation and remagnetization (Elminen et al., 2008; Mertanen et al., 2008). In the case of Satakunta dykes, this is supported by petrophysical and rock magnetic analyses, which show that remanent magnetization values are enhanced and that maghemite is present more often in samples showing component S than in samples showing primary component P, thus favoring hydrothermal origin for the secondary component S.

The secondary remanent magnetization direction similar to component S, with northeasterly declinations, has been widely observed all over the Fennoscandian shield (e.g. Bylund, 1985; Bylund and Elming, 1992; Mertanen and Pesonen, 1995; Mertanen, 2008; Preeden et al., 2009). The direction of this component in Subjotnian formations is always close to PEF direction and usually comes from the most altered dykes. We have plotted secondary poles from Satakunta dykes in Fig. 22 on the Paleozoic apparent polar wander path of Baltica. Normal polarity poles are on the Cambrian part of the APWP, and reversed polarity poles on the early Mesozoic part of the APWP. In the case of the early Mesozoic ages, this component could be related to early stages in the breakup of Pangea supercontinent. If the component had Cambrian age, then it could reflect distal expressions of the Finnmarkian orogeny (Roberts, 2003). Since this component is mainly carried by maghemite, we favor the early Mesozoic age and suggest that it is caused by hydrothermal fluids activated by the break-up of Pangea (see Preeden et al., 2009).

## 6. Conclusions

The studied Subjotnian diabase dykes, associated with rapakivi magmatism in the Satakunta area in Finland, were divided into two groups based on their trends, and paleomagnetic and geochemical results. After removal of a secondary component of possible early Mesozoic age, a two-polarity stable component is revealed in each of the two groups of dykes. Rock-magnetic analyses and positive baked-contact tests indicate that both of these components represent primary thermoremanent magnetizations. The new key pole SK1 (Plat = 29.3°, Plong = 188.1°, $A_{95}$ = 6.6°) was derived from N–S (1565 Ma, Lehtonen et al., 2003) and NE–SW trending dykes, and it fulfills six quality criteria for paleomagnetic poles (Van der Voo, 1990). E–W trending dykes provided primary paleomagnetic pole SK2 (Plat = 32.6°, Plong = 205.5°, $A_{95}$ = 14.3°) that meets five quality criteria. Since the error angles of these poles overlap, paleomagnetism cannot truly distinguish the magnetization ages of these poles. However, the relative position of the poles compared to other well-defined paleomagnetic poles of Baltica indicates that SK2 is older than SK1. Comparison of the new Satakunta poles with the present Mesoproterozoic paleomagnetic data and correlations of geochronology and basement geology for Baltica and Laurentia, suggest that the NENA configuration is valid during the whole time period between 1.8 and 1.2 Ga, forming part of the center of Nuna supercontinent.

## Acknowledgements

Two anonymous reviewers are thanked for their comments to improve the paper. Selen Raiskila, Fredrik Karell and Robert Klein are warmly thanked for their help at the field. Academy of Finland, Yale University, the Foundations' Post Doc Pool, and Otto A. Malm Foundation are thanked for funding JS.

## References

Aouchami, W., Galer, S.J.G., Koschinsky, A., 1999. Pb and Nd isotopes in NE Atlantic Fe–Mn crusts: proxies for trace metal paleosources and paleocean circulation. Geochimica et Cosmochimica Acta 63, 1489–1505.

Åhäll, K.I., Connelly, J., 1998. Intermittent 1.53–1.13 Ga magmatism in western Baltica; age constraints correlations within a postulated supercontinent. Precambrian Research 92, 1–20.

Åhäll, K.I., Connelly, J., Brewer, T.S., 2000. Episodic rapakivi magmatism due to distal orogenies? Correlation of 1.69–1.5 Ga orogenic and inboard anorogenic events in Baltic shield. Geology 28, 823–826.

Andersson, U.B., Eklund, O., Fröjdö, S., Konopelko, D., 2006. 8 Ga magmatism across the Fennoscandian shield; spatial variations in subcontinental mantle enrichment. Lithos 86, 110–136.

Betts, P.G., Giles, D., Schaefer, B.F., 2008. Comparing 1800–1600 Ma accretionary and basin processes in Australia and Laurentia; possible geographic connections in Columbia. Precambrian Research 166, 81–92.

Biggin, A.J., Strik, G.H.M.A., Langereis, C.G., 2008. Evidence for a very-long-term trend in geomagnetic secular variation. Nature Geoscience 1, 395–398.

Bispo-Santos, F., D'Agrella-Filho, M.S., Pacca, I.I.G., Janikian, L., Trindade, R.I.F., Elming, S.-Å., da Silva, J.A., Barros, M.A.S., Pinho, F.M.A.S., 2008. Columbia revisited: paleomagnetic results from the 1790 Ma colider volcanics (SW Amazonian Craton Brazil). Precambrian Research 164, 40–49.

Bispo-Santos, F., D'Agrella-Filho, M.S., Trindade, R.I.F., Elming, S.-Å., Janikian, L., Vasconcelos, P.M., Perillo, B.M., Pacca, I.I.G., da Silva, J.A., Barros, M.A.S., 2012. Tectonic implications of the 1419 Ma Nova Guarita mafic intrusives paleomagnetic pole (Amazonian Craton) on the longevity of Nuna. Precambrian Research 196/197, 1–22.

Borradaile, G.J., Luca, K., Middleton, R.S., 2004. Low-temperature demagnetization isolates stable magnetic vector components in magnetite-bearing diabase. Geophysical Journal International 157, 526–536.

Buchan, K.L., Halls, H.C., 1990. Palaeomagnetism of Proterozoic mafic dyke swarms of the Canadian shield. In: Parker, A.J., Rickwood, P.C., Tucker, D.H. (Eds.), Mafic Dykes and Emplacement Mechanism. Balkema, Rotterdam, pp. 209–230.

Buchan, K.L., Neilson, D.J., Hale, C.J., 1990. Relative age of Otto stock and Matachewan dykes from paleomagnetism and implications for the Precambrian polar wander path. Canadian Journal of Earth Sciences 27, 915–922.

Buchan, K.L., Mertanen, S., Park, R.G., Pesonen, L.J., Elming, S.-Å., Abrahamsen, N., Bylund, G., 2000. Comparing the drift of Laurentia and Baltica in the Proterozoic: the importance of key paleomagnetic poles. Tectonophysics 319, 167–198.

Bylund, G., 1985. Palaeomagnetism of middle Proterozoic basic intrusives in central Sweden and the Fennoscandian apparent polar wander path. Precambrian Research 28, 283–310.

Bylund, G., Elming, S.-Å., 1992. The Dala dolerites, central Sweden, and their palaeomagnetic signature. Geologiska Föreningens i Stockholm Förhandlingar 114, 143–153.

Condie, K.C., 1998. Episodic continental growth and supercontinents: a mantle avalanche connection? Earth and Planetary Science Letters 163, 97–108.

Condie, K.C., 2004. Supercontinents and superplume events: distinguishing signals in the geologic record. Physics of the Earth and Planetary Interiors 146, 319–332.

Day, R., Fuller, M.D., Schmidt, V.A., 1977. Hysteresis properties of titanomagnetites: grain size and composition dependence. Physics of the Earth and Planetary Interiors 13, 260–267.

Dekkers, M.J., 1988. Magnetic properties of natural pyrrhotite. Part I: Behaviour of initial susceptibility and saturation-magnetization-related rock-magnetic parameters in a grain-size dependent framework. Physics of the Earth and Planetary Interiors 52, 376–393.

Dunlop, D.J., 2002. Theory and application of the Day plot (Mrs/Ms versus Hcr/Hc). 1. Theoretical curves and tests using titanomagnetite data. Journal of Geophysical Research 107 (B3), 2056, http://dx.doi.org/10.1029/2001JB000486.

Dunlop, D.J., Özdemir, Ö., 1997. Rock Magnetism: Fundamentals and Frontiers. Cambridge University Press, Cambridge, England, 573 pp.

Ehlers, C., Ehlers, M., 1977. Shearing and multiple intrusion in the diabases of Alandarchipelo, SW Finland. Bulletin of the Geological Survey of Finland 289, 31.

Eklund, O., Shebanov, A., 2005. The prolonged Svecofennian post-collisional shoshonitic magmatism in the southern part of the Svecofennian domain – a case study of the Åva granite – lamprophyre ring complex. Lithos 80, 229–247.

Eklund, O., Fröjdö, S., Lindberg, B., 1994. Magma mixing, the petrogenetic link between anorthositic suites and rapakivi granites, Åland, SW Finland. Mineralogy and Petrology 50, 3–19.

Elminen, T., Airo, M.-L., Niemelä, R., Pajunen, M., Vaarma, M., Wasenius, P., Wennerström, M., 2008. Fault structures in the Helsinki Area, southern Finland. In: Pajunen, M. (Ed.), Tectonic Evolution of the Svecofennian Crust in Southern Finland – A Basis for Characterizing Bedrock Technical Properties. Geological Survey of Finland Special Paper – 47. , pp. 185–213.

Elming, S.-Å., Mattsson, H., 2001. Post Jotnian basic intrusions in the Fennoscandian shield, and the break up of Baltica from Laurentia: a palaeomagnetic and AMS study. Precambrian Research 108, 215–236.

Elming, S.A., Moakhar, M.O., Laye, P., Donadini, F., 2009. Uplift deduced from remanent magnetization of a proterozoic basic dyke and the baked country rock in the Hoting area, Central Sweden: a palaeomagnetic and 40Ar/39Ar study. Geophysical Journal International 179, 59–78.

Emslie, R.F., Irving, E., Park, J.K., 1976. Further paleomagnetic results from the Michikamau intrusion, Labrador. Canadian Journal of Earth Sciences 13, 1052–1057.

Ernst, R.E., Baragar, W.R.A., 1992. Evidence for magnetic fabric for the flow pattern of magma in the Mackenzie giant radiating dyke swarm. Nature 356, 511–513.

Evans, D.A.D., 2006. Proterozoic low orbital obliquity and axial-dipolar geomagnetic field from evaporate palaeolatitudes. Nature 444, 51–55.

Evans, D.A.D., Pisarevsky, S.A., 2008. Plate Tectonics on Early Earth? Weighing the Paleomagnetic Evidence. Geological Society of America Special Paper 440., pp. 249–263.

Evans, D.A.D., Mitchell, R.N., 2011. Assembly and breakup of the core of Paleo-Mesoproterozoic supercontinent Nuna. Geology 39, 443–446.

Everitt, C.W.F., Clegg, J.A., 1962. A field test of paleomagnetic stability. Geophysical Journal of the Royal Astronomical Society 6, 312–319.

Fisher, R., 1953. Dispersion of a sphere. Proceedings of the Royal Society of London 217, 295–305.

Gower, C.F., Ryan, A.B., Rivers, T., 1990. Mid-Proterozoic Laurentia–Baltica: an overview of its geological evolution and a summary of the contributions made by this volume. In: Gower, C.F., Rivers, T., Ryan, B. (Eds.), Mid-Proterozoic Laurentia–Baltica. Geological Association of Canada Special Paper 38, pp. 1–20.

Haapala, I., Rämö, T.O., 1992. Tectonic setting and origin of the Proterozoic rapakivi granites of southeastern Fennoscandia. Transactions of the Royal Society of Edinburgh Earth Sciences 83, 65–171.

Haapala, I., Rämö, T.O., Frindt, S., 2005. Comparison of Proterozoic and Phanerozoic rift-related basaltic-granitic magmatism. Lithos 80, 1–32.

Halls, H.C., Li, J., Davis, D., Hou, G., Zhang, B., Qian, X., 2000. A precisely dated Proterozoic palaeomagnetic pole for the North China craton, and its relevance to palaeocontinental reconstruction. Geophysical Journal International 143, 185–203.

Halls, H.C., Hamilton, M., Denyszyn, S.W., 2011. The Melville Bugt dyke swarm of Greenland: a connection to the 1.5–1.6 Ga Fennoscandian rapakivi granite province? In: Srivastava (Ed.), Dyke Swarms: Keys for Geodynamic Interpretation. , pp. 509–535, http://dx.doi.org/10.1007/987-3-642-12496-9_27.

Hamilton, M., Buchan, A.K.L., 2010. U–Pb geochronology of the Western Channel Diabase, northwestern Laurentia: implications for a large 1.59 Ga magmatic province Laurentia's APWP and paleocontinental reconstructions of Laurentia, Baltica and Gawler craton of southern Australia. Precambrian Research 183, 463–473.

Hart, S.R., Blusztajn, J.S., 2006. Age and geochemistry of the mafic sills, ODP site 1276, Newfoundland margin. Chemical Geology 235, 222–237.

Hoffman, P.F., 1989. Precambrian geology and tectonic history of North America. In: Bally, A.W., Palmer, A.R. (Eds.), The Geology of North America. Geological Society of America, Boulder, CO, pp. 447–512.

Hoffman, P.F., 1991. Did the breakout of Laurentia turn Gondwana inside out? Science 252, 1409–1412.

Hoffman, P.F., 1996. Tectonic genealogy of North America. In: Van der Pluijm, B.A., Marshak, S. (Eds.), Earth Structure: An Introduction to Structural Geology and Tectonics. McGraw-Hill, New York, pp. 459–464.

Hospers, J., 1954. Rock magnetism and polar wandering. Nature 173, 1183–1184.

Hrouda, F., 1982. Magnetic anisotropy of rocks and its application in geology and geophysics. Geophysical Surveys 5, 37–82.

Huhma, H., 1986. Sm–Nd, U–Pb, and Pb–Pb isotopic evidence for the origin of the Early Proterozoic Svecokarelian crust in Finland. Geological Survey of Finland, Bulletin 337, 1–48.

Irving, E., 1964. Paleomagnetism and its Application to Geological and Geophysical Problems. John Wiley, New York, 399 pp.

Irving, E., 2005. The role of latitude in mobilism debates. Proceedings of the National Academy of Sciences of the United States of America 102, 1821–1828.

Irving, E., Donaldson, J.A., Park, J.K., 1972. Paleomagnetism of the Western Channel diabase and associated rocks, Northwest Territories. Canadian Journal of Earth Sciences 9, 960–971.

Irving, E., Baker, J., Hamilton, M., Wynne, P.J., 2004. Early Proterozoic geomagnetic field in western Laurentia: implications for paleolatitudes, local rotations and stratigraphy. Precambrian Research 129, 251–270.

Jelinek, V., 1981. Characterization of the magnetic fabric of rocks. Tectonophysics 79, T63–T67.

Johansson, Å., 2009. Baltica Amazonia and the SAMBA connection – 1000 million years of neighbourhood during the Proterozoic? Precambrian Research 175, 221–234.

Jones, C.H., 2002. User-driven integrated software lives: "PaleoMag" Paleomagnetics analysis on the Macintosh. Computers & Geosciences 28, 1145–1151.

Karlstrom, K.E., Åhäll, K.-I., Harlan, S., Williams, M.L., McLelland, J., Geissman, J.W., 2001. Long-lived (1.8–1.0 Ga) covergent orogen in southern Laurentia, its extensions to Australia and Baltica, and implications for refining Rodinia. Precambrian Research 111, 5–30.

Kirschvink, J.L., 1980. The least-squares line and plane and the paleomagnetic data. Geophysical Journal of the Royal Astronomy Society 62, 699–718.

Kirschvink, J.L., Kopp, R.E., Raub, T.D., Baumgartner, C.T., Holt, J.W., 2008. Rapid, precise, and high-sensitivity acquisition of paleomagnetic and rock-magnetic data: development of a low-noise automatic sample changing system for superconducting rock magnetometers. Geochemistry, Geophysics, Geosystems 9, Q05Y01, http://dx.doi.org/10.1029/2007GC001856.

Klein, R., Pesonen, S., Salminen, L.J., Mertanen, J., 2013. Paleomagnetic study of Mesoproterozoic Satakunta sandstone, Western Finland. Precambrian Research (in this volume).

Knight, M.D., Walker, G.P.L., 1988. Magma flow directions in dikes of the Koolau complex, Oahu, determined from magnetic fabric studies. Journal of Geophysical Research 93, 4301–4319.

Korja, A., Lahtinen, R., Nironen, M., 2006. The Svecofennian Orogen: A Collage of Microcontinents and Islands Arcs. Geological Society of London Memoir 32., pp. 561–578.

Korsman, K., Koistinen, T., Kohonen, J., Wennerström, M., Ekdahl, E., Honkamo, M., Idman, H., Pekkala, Y. (Eds.), 1997. Bedrock Map of Finland 1:1000000. Geol. Surv. Fin. Espoo, Finland.

Kusky, T.M., Li, J., Santosh, M., 2007. The Paleoproterozoic North Hebei Orogen: North china cratons collisional structure with Columbia supercontinent. Gondwana Research 12, 4–28.

Lahtinen, R., Garde, A.A., Melezhik, V.A., 2008. Paleoproterozoic evolution of Fennoscandia and Greenland. Episodes 31, 20–28.

Laitakari, I., 1987. The Subjotnian diabase dyke swarm of Hame. In: Aro, K., Laitakari, I. (Eds.), Suomen diabaasit ja muut mafiset kivilajit. Geological Survey of Finland Report of Investigation 76. , pp. 99–116.

Larin, A.M., 2009. Rapakivi granites in the geological history of the Earth. Part 1. Magnetic associations with rapakivi granites: age, geochemistry, and tectonic setting. Stratigraphy and Geological Correlation 17, 3–28 (translated from Russia).

Lehtonen, M.I., Kujala, H., Kärkkäinen, N., Lehtonen, A., Mäkitie, H., Mänttäri, I., Virransalo, P., Vuokko, J., 2003. Etelä-Pohjanmaan liuskealueen kallioperä. Summary: Pre-Quaternary Rocks of the South Ostrobothnian Schist Belt. Geological Survey of Finland Report of Investigation 158., pp. 125.

Lindberg, B., Eklund, O., 1992. Mixing between basaltic and granitic magmas in a rapakivirelated quartz-feldspar porphyry, Åland, SW Finland. Geologiska Föreningens i Stockholm Förhandlingar (GFF) 114, 103–112.

Lubnina, N.V., Mertanen, S., Soderlund, U., Bogdanova, S., Vasilieva, T.T., Frank-Kamenetsky, D., 2010. A new key pole for the east European craton at 1452 Ma: Paleomagnetic and geochronological constraints from mafic rocks in Lake Ladoga region (Russian Karelia). Precambrian Research 183, 442–462.

Luttinen, A.V., Kosunen, P.J., 2006. The Kopparnäs dyke swarm in Inkoo, southern Finland: new evidence for Jotnian magmatism in the SE Fennoscandian Shield. In: Hanski, E., Mertanen, S., Rämö, T., Vuollo, J. (Eds.), Dyke Swarms – Time Markers of Crustal Evolution. Selected Papers of the Fifth International Dyke Conference in Finland. Rovaniemi, Finland, 31 July–3 August 2005. Taylor & Francis Group, London, pp. 85–97.

Mänttäri, I., Paulamäki, S., Suominen, V., 2005. U–Pb Age Constraints for the Diabase Dyke from Investigation Trench OL-TK3 at the Olkiluoto Study Site, Eurajoki, SW Finland. Posiva. Working Report 2004-67. Posiva, Olkiluoto, 18 pp.

McFadden, P.L., McElhinney, M.W., 1990. Classification of the reversal test in palaeomagnetism. Geophysical Journal International 103, 725–729.

Meert, J.G., 2002. Paleomagnetic evidence for a Paleo-Mesoproterozoic supercontinent Columbia. Gondwana Research 5, 207–215.

Meert, J.G., Stuckey, W., 2002. Revisiting the paleomagnetism of the 1.476 Ga St. Francois Mountains igneous province, Missouri. Tectonics 21, http://dx.doi.org/10.1029/2000TC001265.

Mertanen, S., 2008. Paleomagnetism of Diabase Dykes, Pegmatitic Granites and TGG Gneisses in the Olkiluoto Area. Working Report 2007-96. Posiva, Olkiluoto, 35 pp.

Mertanen, S., Pesonen, L.J., 1995. Paleomagnetic and rock magnetic investigations of the Sipoo Subjotnian quartz porphyry and diabase dykes, southern Fennoscandia. Physics of the Earth and Planetary Interiors 88, 145–175.

Mertanen, S., Airo, M.-L., Elminen, T., Niemelä, R., Pajunen, M., Wasenius, P., Wennerström, M., 2008. Paleomagnetic evidence for Mesoproterozoic – Paleozoic reactivation of the Paleoproterozoic crust in southern Finland. In: Pajunen, M. (Ed.), Tectonic Evolution of the Svecofennian Crust in Southern Finland – A Basis for Characterizing Bedrock Technical Properties. Geological Survey of Finland Special Paper 47, pp. 215–252.

Merrill, R.T., McElhinny, M.W., 1983. The Earth's Magnetic Field: Its History, Origin, and Planetary Perspective. Academic Press, London, 401 pp.

Moakhar, M.O., Elming, S.-Å., 2000. A Palaeomagnetic analysis of Rapakivi intrusions and related dykes in the Fennoscandian Shield. Physics and Chemistry of the Earth, Part A 25 (6), 489–494.

Neuvonen, K.J., 1967. Paleomagnetism of the dike systems in Finland – III. Remanent magnetization of diabase dyke in Hame, Finland. Comptes Rendus de la Société géologique de Finlande 39, 87–94.

Neuvonen, K.J., 1970. Remanent magnetization of the Åva intrusives. Bulletin of the Geological Society of Finland 42, 101–107.

Neuvonen, K.J., 1978. Remanent magnetization of two intrusive bodies in southeastern Finland. Bulletin of the Geological Society of Finland 50, 31–37.

Neuvonen, K.J., 1986. On the direction of remanent magnetization of the quartz porphyry dikes in SE Finland. Bulletin of the Geological Society of Finland 58, 195–201.

Neuvonen, K.J., Grundström, L., 1969. Palaeomagnetism of the dike systems in Finland IV Remanenet magnetization of the dolerite and related dikes in the Åland archipelago. Bulletin of the Geological Society of Finland 41, 57–63.

Onstott, T.C., 1980. Application of the Bingham distribution function in paleomagnetic studies. Journal of Geophysical Research 85, 1500–1510, http://dx.doi.org/10.1029/JB085iB03p01500.

O'Reilly, W., 1984. Rock and Mineral Magnetism. Blackie, Glasgow, 220 pp.

Parés, J.M., Van der Voo, R., 2013. Non-antipodal directions in magnetostratigraphy: an overprint bias? Geophysical Journal International 192, 75–81.

Park, J.K., Irving, E., Donaldson, J.A., 1973. Paleomagnetism of the Dubawnt Group. Geological Society of America Bulletin 84, 859–870.

Patchett, P.J., Bylund, G., Upton, B.G.J., 1978. Palaeomagnetism and the Grenville orogeny: new Rb–Sr ages from dolerites in Canada and Greenland. Earth and Planetary Science Letters 40, 349–364.

Paulamäki, S., Paananen, M., Gehör, S., Kärki, A., Front, K., Aaltonen, I., Ahokas, T., Kemppainen, K., Mattila, J., Wikström, L., 2006. Geological Model of the Olkiluoto Site, Version 1.0. Working Report 2006-37. Posiva Oy, Eurajoki, 355 pp.

Payne, J.L., Hand, M., Barovich, K.M., Reid, A., Evans, D.A.D., 2009. Correlations and reconstruction models for the 2500–1500 Ma evolution of the Mawson Continent. In: Reddy, S.M., Mazumder, R., Evans, D.A.D., Collins, A.S. (Eds.), Palaeoproterozoic Supercontinents and Global Evolution. Geological Society of London Special Publication 323, pp. 319–355.

Pesonen, L.J., 1987. On the paleomagnetism of mafic dykes in Finland. In: Aro, K., Laitakari, I. (Eds.), Diabases and Other Mafic Dyke Rocks in Finland, Rep. Invest. 76, Geological Survey of Finland Espoo. , pp. 205–220 (in Finnish with English abstract).

Pesonen, L.J., Neuvonen, K.J., 1981. Palaeomagnetism of the Baltic Shield – implications for Precambrian tectonics. In: Kroner, A. (Ed.), Developments in Precambrian Geology, 4, pp. 623–648.

Pesonen, L.J., Suominen, V.O., Noras, P.,1987. Paleomagnetism of the Subjotnian diabase dyke swarms of the Åland Archipelago, SE-Finland. In: International Conference on Mafic Dyke Swarms, Abstract. University of Toronto, pp. 129–130.

Pesonen, L.J., Bylund, G., Torsvik, T.H., Elming, S.-Å., Mertanen, S., 1991. Catalogue of paleomagnetic directions and poles from Fennoscandia: Archaean to Tertiary. Tectonophysics 195, 151–207.

Pesonen, L.J., Elming, S.-Å., Mertanen, S., Pisarevsky, S., D'Agrella-Filho, M.S., Meert, J.G., Schmidt, P.W., Abrahamsen, N., Bylund, G., 2003. Paleomagnetic configuration of continents during the Proterozoic. Tectonophysics 375, 289–324.

Pesonen, L.J., Mertanen, S., Veikkolainen, T.H.K., 2012. Paleo-Mesoproterozoic supercontinents – a Paleomagnetic view. Geophysica 48, 5–47.

Pihlaja, 1987. Porin seudun subjotuniset diabaasit. Abstract: the Subjotnian diabases of the Pori region, southwestern Finland. In: Aro, K., Laitakari, I. (Eds.), Suomen diabaasit ja muut mafiset juonikivilajit. Geological Survey of Finland Report of Investigation 76, pp. 133–150.

Piper, J.D.A., 1979. A palaeomagnetic survey of the Jotnian dolerites of central-east Sweden. Geophysical Journal of the Astronomical Society 56, 461–471.

Piper, J.D.A., 1980. Analogous Upper Proterozoic apparent polar wander loops. Nature 283, 845–847.

Piper, J.D.A., 1992. Palaeomagnetism of the Almunge alkaline complex and Tuna dykes, Sweden; Mid-Proterozoic palaeopoles from the Fennoscandian Shield. Geologiska Föreningens i Stockholm Förhandlingar 114, 291–297.

Pisarevsky, S.A., Sokolov, S.J., 1999. Palaeomagnetism of the Palaeoproterozoic ultramafic intrusion near Lake Konchozero, Southern Karelia, Russia. Precambrian Research 93, 201–213.

Pisarevsky, S.A., Sokolov, S.J., 2001. The magnetostratigraphy and a 1780 Ma palaeomagnetic pole from the red sandstones of the Vazhinka River section, Karelia, Russia. Geophysical Journal International 146, 531–538.

Pisarevsky, S.A., Bylund, G., 2010. Paleomagnetism of 1780–1770 Ma mafic and composite intrusions of Småland (Sweden): implications for the mesoproterozoic supercontinent. American Journal of Science 310, 1168–1186.

Preeden, U., Mertanen, S., Elminen, T., Plado, J., 2009. Secondary magnetizations in shear and fault zones in southern Finland. Tectonophysics 479, 203–213.

Raiskila, S., Salminen, J., Elbra, T., Pesonen, L.J., 2011. Rock magnetic and paleomagnetic study of the Keurusselkä impact structure, central Finland. Meteoritics and Planetary Science 46, 1670–1687.

Rämö, O.T., 1991. Petrogenesis of the Proterozoic rapakivi granites and related basic rocks of southeastern Fennoscandia: Nd and Pb isotopic and general geochemical constraints. Bulletin of the Geological Survey of Finland 355, 1–161.

Rämö, O.T., Haapala, I., 1995. One hundred years of rapakivi granite. Contributions to Mineralogy and Petrology 52, 129–185.

Rämö, O.T., Mänttäri, I., Kohonen, J., Upton, B.G.J., Luttinen, A.V., Lindqvist, V., Lobaev, V.M., Cuney, M., Sviridenko, L.P., 2005. Mesoproterozoic CFB magmatism in the Lake Ladoga basin, Russian Karelia. In: Vuollo, J., Mertanen, S. (Eds.), Fifth International Dyke Conference. 31 July–3 August, 2005, Rovaniemi, Finland. Abstracts and Programme, pp. 41–42.

Raposo, M.I.B., 2011. Magnetic fabric of the Brazilian Dike Swarms: a review. In: Petrovský, E., Ivers, D., Harinarayana, T., Herrero-Bervera, E. (Eds.), The Earth's Magnetic Interior. IAGA Special Sopron Book Series, vol. 1, pp. 247–262, http://dx.doi.org/10.1007/978-94-007-0323-0_17.

Raposo, M.I.B., Chaves, A.O., Lojkasek-Lima, P., D'Agrella-Filho, M.S., Teixeira, W., 2004. Magnetic fabrics and rock magnetism of Proterozoic dike swarm from the southern São Francisco Craton, Minas Gerais State, Brazil. Tectonophysics 378, 43–63.

Reddy, S.M., Evans, D.A.D., 2009. Palaeoproterozoic supercontinents and global evolution: correlations from core to atmosphere. In: Reddy, S.M., Mazumder, R., Evans, D.A.D., Collins, A.S. (Eds.), Palaeoproterozoic Supercontinents and Global Evolution. Geological Society of London Special Publications 323, pp. 1–26.

Roberts, D., 2003. The Scandinavian Caledonides: event chronology, palaeogeographic settings and likely modern analogues. Tectonophysics 365, 283–299.

Rochette, P., Jackson, M.J., Aubourg, C., 1992. Rock magnetism and the interpretation of anisotropy of magnetic susceptibility. Reviews of Geophysics 3, 209–226.

Rochette, P., Aubourg, C., Perrin, M., 1999. Is this magnetic fabric normal? A review and case studies in volcanic formations. Tectonophysics 307, 219–234.

Roest, E.R., Sirvastava, S.P., 1989. Sea floor spreading in the Labrador Sea: a new reconstruction. Geology 17, 1000–1003.

Rogers, J.J.W., Santosh, M., 2002. Configuration of Columbia, a Mesoproterozoic supercontinent. Gondwana Research 5, 5–22.

Salminen, J., Pesonen, L.J., 2007. Paleomagnetic and rock magnetic study of the Mesoproterozoic sill, Valaam island, Russian Karelia. Precambrian Research 159, 212–230.

Salminen, J., Pesonen, L.J., Mertanen, S., Vuollo, J., Airo, M.L., 2009. Palaeomagnetism of the Salla Diabase Dyke, northeastern Finland, and its implication to the Baltica – Laurentia entity during the Mesoproterozoic. In: Reddy, S.M., Mazumder, R., Evans, D.A.D., Collins, A.S. (Eds.), Palaeoproterozoic Supercontinents and Global Evolution. Geological Society London Special Publications 323, pp. 199–217.

Smirnov, A., Tarduno, J., Evans, D.A.D., 2011. Evolving core conditions ca. 2 billion years ago detected by paleosecular variation. Physics of the Earth and Planetary Interiors 187, 225–231.

Suominen, V., 1991. The Chronostratigraphy of South-Western Finland with Special Reference to Postjotnian and Subjotnian Diabases. Geological Survey of Finland Bulletin 356, 100 pp.

Shcherbakova, V.V., Pavlov, V.E., Shcherbakov, V.P., Neronov, I., Zemtsov, V.A., 2006. Palaeomagnetic studies and estimation of geomagnetic palaeointensity at the Early/Middle Riphean boundary in rocks of the Salmi formation (north Ladoga area). Izvestiya Physics Solid Earth 42, 233–243.

Shebanov, A., Savatenkov, V., Eklund, O., Andersson, U.B., Annersten, H., Claesson, S., 2000. Regional mineralogical correlation linking post- and anorogenic magmatic events from unusual barian biotites in the Järppilä rapakivi porphyries, Vehmaa batolith (S. Finland). In: Meeting: Advances on Micas Rome 2–3.11 2000. Universitá degli Studi Roma Tre MURST – Progetto Fillosilicati: aspetti cristallochimici strutturali e petrologici, pp. 183–186.

Smirnov, A.V., Tarduno, J.A., 2004. Secular variation of the Late Archean–Early Proterozoic geodynamo. Geophysical Research Letters 31, L16607.1–L16607.4.

Suominen, V, Fagerström, Pi, Torssonen, M, 2006. Uudenkaupungin kartta-alueen kallioperä. Summary: Pre-Quaternary rocks of the Uusikaupunki map-sheet area. Geological Survey of Finland 89 p. + 2 app. maps.

Tauxe, L., Gee, J.S., Staudigel, H., 1998. Flow directions in dikes from anisotropy of magnetic susceptibility data: the bootstrap way. Journal of Geophysical Research 103, 17775–17790.

Torsvik, T.H., Smethurst, M.A., Van der Voo, R., Trench, A., Abrahamsen, N., Halvorsen, E., 1992. Baltica – a synopsis of Vendian-Permian palaeomagnetic data and their palaeotectonic implications. Earth-Science Reviews 33, 133–152.

Torsvik, T.H., Smethurst, M.A., Meert, J.G., Van der Voo, R., McKerrow, W.S., Brasier, M.D., Sturt, B.A., Walderhaug, H.J., 1996. Continental break-up and collision in the Neoproterozoic and Palaeozoic: a tale of Baltica and Laurentia. Earth-Science Reviews 40, 229–258.

Vaasjoki, Sakko, 1989. The radiometric age of the Virmaila diabase dyke: evidence for 20 Ma continental rifting in Padasjoki, southern Finland. In: Autio, S. (Ed.), Currents Research 1988, Geological Survey of Finland Special Paper 10, pp. 43–44.

Vaasjoki, M., Rämö, T.O., Sakko, M., 1991. New U–Pb ages from the Wiborg rapakivi area: constraints on the temporal evolution of the rapakivi granite-anorthosite-diabase dyke association of southeastern Finland. Precambrian Research 51, 227–243.

Van der Voo, R., 1990. The reliability of paleomagnetic data. Tectonophysics 184, 1–9.

Williams, H., Hoffman, P.F., Lewry, J.F., Monger, J.W.H., Rivers, T., 1991. Anatomy of North America: thematic portrayals of the continent. Tectonophysics 187, 117–134.

Wingate, M.T.D., Pisarevsky, S.A., Gladkochub, D.P., Donskaya, T.V., Konstantinov, K.M., Mazukabzov, A.M., Stanevich, A.M., 2009. Geochronology and paleomagnetism of mafic igneous rocks in the Olenëk Uplift, northern Siberia: implications for Mesoproterozoic supercontinents and paleogeography. Precambrian Research 170, 256–266.

Wu, H., Zhang, S., Li, Z.-X., Li, H., Dong, J., 2005. New paleomagnetic results from the Yangzhuang Formation of the Jixian System, north China, and tectonic implications. Chinese Science Bulletin 50, 1483–1489.

Zhang, S., Li, Z.-X., Evans, D.A.D., Wu, H., Li, H., Dong, J., 2012. Pre-Rodinia supercontinent Nuna shaping up: a global synthesis with new paleomagnetic results from North China. Earth and Planetary Science Letters 353/354, 145–155.

Zhao, G., Cawood, P.A., Wilde, S.A., Sun, M., 2002. Review of global 2.1–1.8 Ga orogens: implications for a pre-Rodinia supercontinent. Earth-Science Reviews 59, 125–162.

Zhao, G., Sun, M., Wilde, S.A., Li, S., 2004. A Paleo-mesoproterozoic supercontinent: assembly, growth and breakup. Earth-Science Reviews 67, 91–123.

Zijderveld, J.D., 1967. A.C. demagnetization in rocks: analysis of results. In: Collinson, D.W., Creer, K.M., Runcorn, S.K. (Eds.), Methods in Paleomagnetism. Elsevier, New York, pp. 254–286.